BOEING

CR-151665

D180-22876-1

NAS9-15196
DRL T-1346
DRD MA-664T
LINE ITEM 3

Volume I
Executive Summary

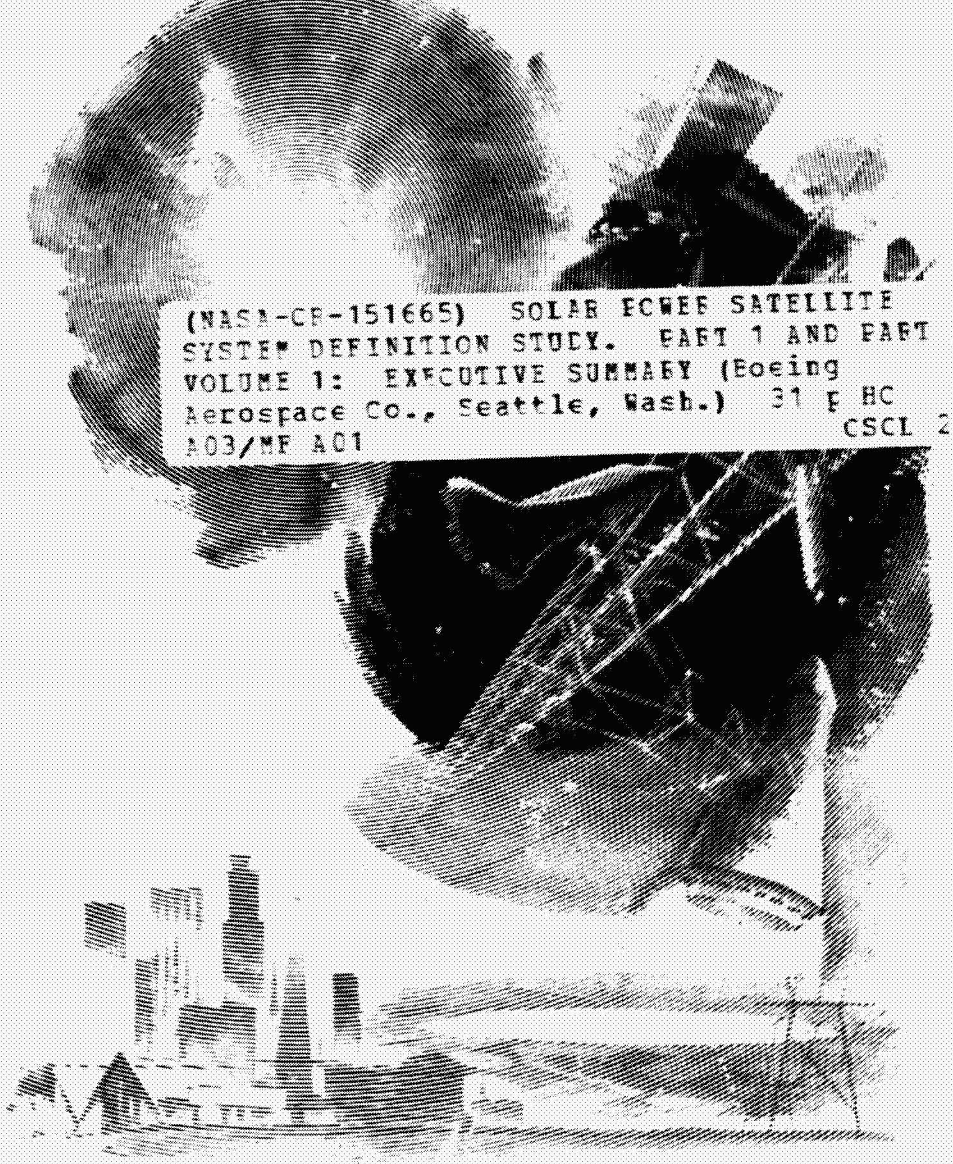

(NASA-CR-151665) SOLAR POWER SATELLITE SYSTEM DEFINITION STUDY. PART 1 AND PART 2, VOLUME 1: EXECUTIVE SUMMARY (Boeing Aerospace Co., Seattle, Wash.) 31 p HC A03/MF A01 CSCL 22B G3/15 N78-20162 Unclas 11820

Solar Power Satellite

SYSTEM DEFINITION STUDY
PART I AND PART II

D180-22876-1

CONTRACT NAS9-15196
DRL T-134-6
DRD MA-664T
LINE ITEM 3

Solar Power Satellite

SYSTEM DEFINITION STUDY PART I AND PART II

VOLUME I

EXECUTIVE SUMMARY

D180-22876-1

December 1977

Submitted To
The National Aeronautics and Space Administration
Lyndon B. Johnson Space Center
in Fulfillment of the Requirements
of Contract NAS9-15196

Approved: G. R. Woodcock

G. R. Woodcock
Study Manager

BOEING AEROSPACE COMPANY
MISSILES AND SPACE GROUP–SPACE DIVISION
P.O. BOX 3999
SEATTLE, WASHINGTON

FOREWORD

The SPS systems definition study was initiated in December 1976. Part I was completed on May 1, 1977. Part II technical work was completed October 31, 1977.

The study was managed by the Lyndon B. Johnson Space Center (JSC) of the National Aeronautics and Space Administration (NASA). The Contracting Officer's Representative (COR) was Clarke Covington of JSC. The study was performed by the Boeing Aerospace Company. The Boeing study manager was Gordon Woodcock. Boeing Commercial Airplane Company assisted in the analysis of launch vehicle noise and overpressures.

The General Electric Company Space Division was the major subcontractor for the study. Their contributions included Rankine cycle power generation, power processing and switchgear, microwave transmitter phase control and alternative transmitter configurations, remote manipulators, and thin-film silicon photovoltaics.

Other subcontractors were Hughes Research Center–gallium arsenide photovoltaics; Varian–klystrons and klystron production; SPIRE–silicon solar cell directed energy annealing.

This report was prepared in 8 volumes as follows:

- I – Executive Summary
- II – Technical Summary
- III – SPS Satellite Systems
- IV – Microwave Power Transmission Systems
- V – Space Operations
- VI – Evaluation Data Book
- VII – Study Part II Final Briefing Book
- VIII – SPS Launch Vehicle Ascent and Entry Sonic Overpressure and Noise Effects

TABLE OF CONTENTS

LIST OF FIGURES

LIST OF TABLES

INTRODUCTION

Solar power satellites offer a potentially economic means of producing solar baseload electric power for commercial use in any desired amount. The energy source—sunlight—will be available for billions of years.

The solar power satellite (SPS) principle is illustrated in Figures 1 and 2. In a geostationary orbit 36 000 km above the Earth's equator, each SPS is in sunlight over 99% of the time and in continuous line-of-sight contact with its ground receiving station. Electrical power produced on the satellite by photovoltaic (solar cell) or heat engine (turbogenerator) conversion of sunlight is then converted to radio frequency energy at high efficiency, and formed into a focused beam precisely aimed at the SPS ground stations. The ground station receiving antenna reconverts the energy into electricity for distribution.

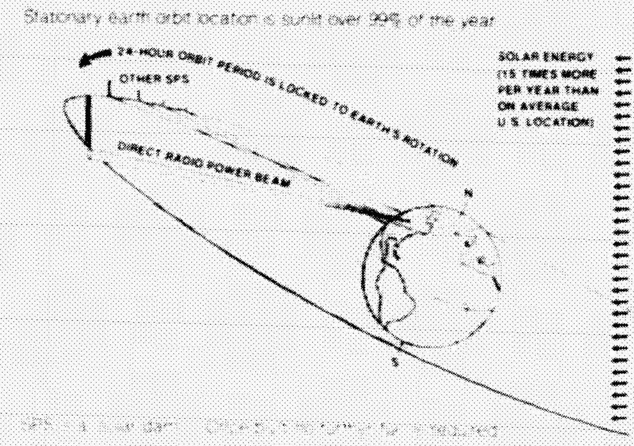

Figure 2. The Principle of SPS

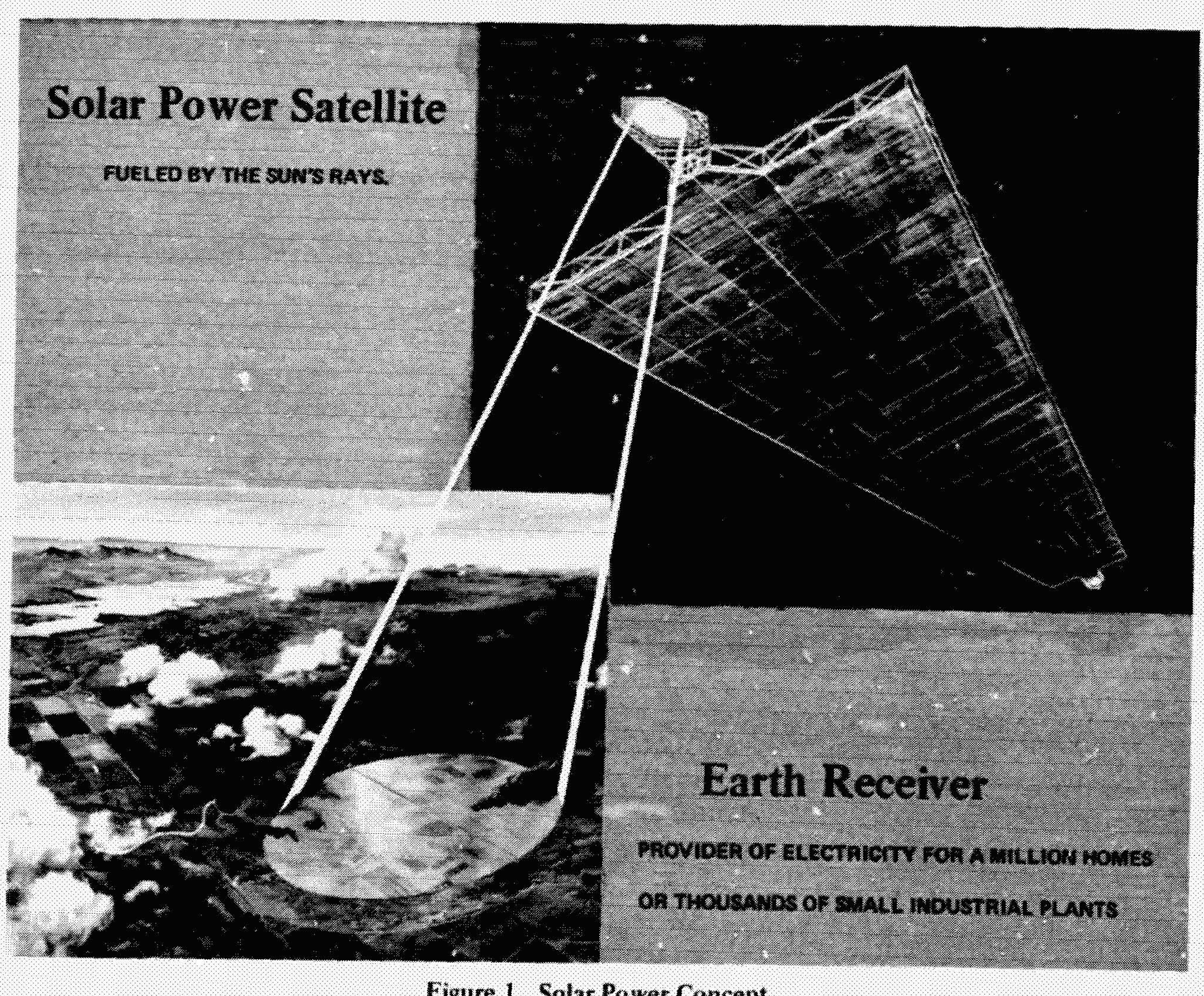

Figure 1. Solar Power Concept

The solar power satellite concept was originated about ten years ago by Dr. Peter Glaser. The concept was initially not taken seriously by most of the technical community, but was investigated by NASA through some small contracted studies in 1971 and 1972. These studies confirmed basic technical feasibility of the idea. Strong objections were raised, however, primarily that: (1) efficient long-range wireless energy transmission was not possible, and (2) the space flight operations required to install SPS's in their operational orbit would be hopelessly expensive.

Further studies and experiments funded by NASA over the period 1973-1975 all but abolished doubt of the feasibility of efficient wireless energy transmissions at microwave frequencies (2450 Mhz). The *experimentum crucis* was conducted at JPL in 1975; more than 30 kilowatts was transmitted across a distance of more than a mile with reception and conversion efficiency of 82% (Figure 3).

The space flight cost issue has not been so easily resolved. Space transportation cost per unit mass delivered to a low Earth orbit has been used as a primary figure of merit and is the focal point of the controversy. Transportation cost studies by Boeing, under the Future Space Transportation Systems Analysis (FSTSA) study, in 1974-75 indicated that SPS economic feasibility depended on achieving a cost below \$50/kg and that such costs were almost certainly attainable. (By way of comparison, current costs are \$2000/kg or more, and Space Shuttle user charges will probably average on the order of \$500/kg.) Transportation system studies in the 1975-76 period projected costs in the \$10/kg-\$35/kg range for SPS operations, but doubts persist in the minds of many knowledgeable people even today.

Increased interest in the SPS idea led to new studies in the 1975-76 period with emphasis on (a) economic evaluation (NASA-MSFC/ECON-Grumman), (b) Alternatives to silicon solar cell

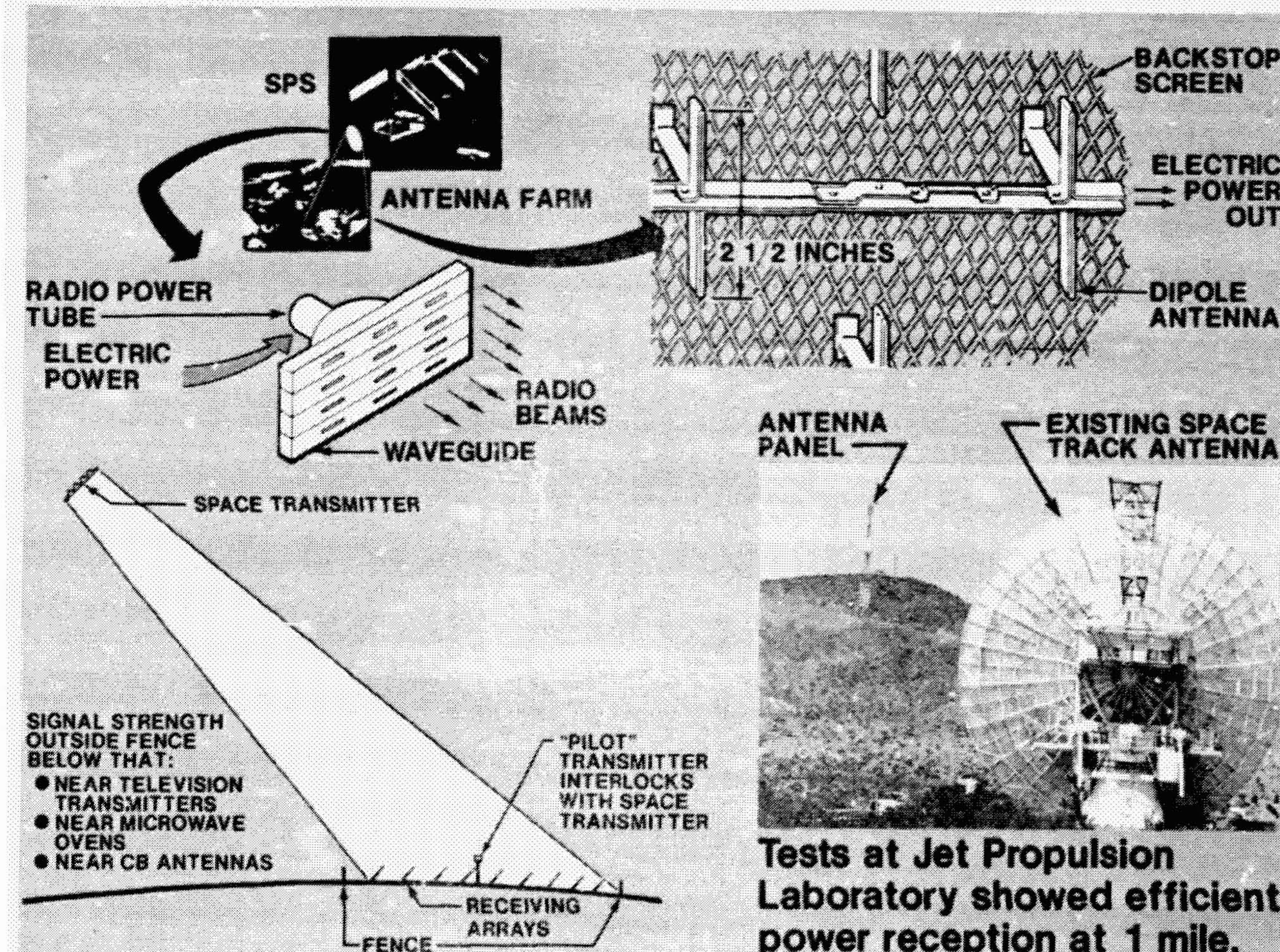

Figure 3. Energy Can Be Efficiently Transported By Radio Beam

energy conversion (NASA-MSFC/Boeing), and (c) better definition of a reference or baseline silicon photovoltaic system concept (NASA-JSC inhouse). More or less concurrently, continuing analytical and experimental activities aimed at improving knowledge of the power transmission technology were funded by NASA-Lewis Research Center with JPL and Raytheon. Up to this time, essentially all of the power transmission studies had emphasized the amplitron cross-field amplifier as a DC/RF converter. The JSC inhouse effort, however, emphasized the Klystron linear beam tube.

In late 1976, the situation could be summarized as follows:

(1) Energy conversion studies had concentrated on silicon photovoltaic and Brayton (closed cycle gas turbine) power generation. Initial studies of gallium arsenide photovoltaics, primarily by Rockwell, indicated significant potential advantages. Other possible options such as Rankine vapor cycles and thin-film photovoltaics, had not been investigated. No systematic comparative evaluation had been conducted.

(2) A controversy of sorts had developed over space operations options. The most straightforward approach to SPS installation is to transport the flight hardware to geosynchronous orbit (GEO) and construct the SPS's there at the operational location. An alternative advanced by Boeing was to construct the SPS's in a low Earth orbit (LEO) and use their power generating capability to drive them to GEO by electric rocket propulsion. This option exhibited potential cost savings but several operational issues had not been investigated.

(3) Almost all the power transmission analyses had been based on amplitron RF power tubes. The JSC inhouse effort, however, indicated the Klystron to have significant potential advantages.

(4) Only the most cursory explorations of construction of these large objects in space had been conducted.

(5) Transportation system studies had been predominantly parametric and considered the SPS application only as one of many, although the same studies had indicated the SPS requirement to be unique. Issues such as payload packaging and integrated operations were not understood.

The SPS systems study work statements and plans were to provide for an effort more comprehensive and in greater depth than the earlier work, and were intended to achieve a major reduction in technical and economic uncertainties regarding the SPS concept and its potential application to mankind's energy needs.

STUDY DESCRIPTION

The overall plan developed by JSC called for conduct of the study in two parts. Part I, conducted from Dec. 1976 through April 1977, was to concentrate on the first two issues described above: What is the best specific means of energy conversion, and where (LEO or GEO) should the space construction operations take place?

With these issues resolved to the degree practicable, Part II of the study, conducted from May through November, 1977, was to concentrate on development of an end-to-end system definition with emphasis on assessment of, and reduction in, system mass and cost uncertainties.

SYNOPSIS OF STUDY RESULTS

Findings

The most significant study results are summarized below. The study concentrated on maximum confidence system designs with the result that the SPS, rather than being a mid-21st-century system, should be achievable by the year 2000, and could be economically attractive as shown in Figure 4. The base technology is in hand. After a modest technology verification effort of 3 to 5 years duration, *full scale development could begin* and would provide a mainstream energy system of great potential.

Power Transmission
- Basic Feasibility Confirmed
- Detailed Microwave Link Error Analysis Confirmed Attainability of Adequate Efficiency

Energy Conversion
- Silicon Photovoltaic Best Overall Choice
- Potassium Rankine Backup Choice

Space Transportation Operations
- Low Cost Due To Traffic Level, Not New Technology
- Payload Volume is Launch Vehicle Design Driver

SPS System Costs
- Power Cost 4 to 5¢/kwh; Competitive with Fossil Sources by Year 2000
- System Design Flexibility Key To Cost Confidence

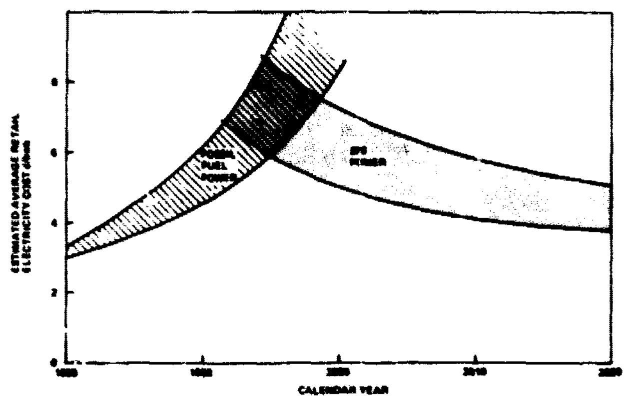

Figure 4. Projections Indicate SPS Power Will Be Economically Attractive

STUDY ACCOMPLISHMENTS AND RESULTS

Part I Issues

Energy Conversion

The evaluation effort included all energy conversion options known to be of potential interest for the SPS applications:

(1) Silicon single crystal photovoltaics;
(2) Gallium arsenide single crystal and thin-film photovoltaics;
(3) Other thin-film photovoltaics;
(4) Thermal engine Rankine closed-cycle vapor turbines, with several working fluids under consideration;
(5) Thermal engine Brayton closed cycle gas turbines;
(6) Thermionic direct thermal conversion.

Certain known options were not included:

(1) Thermoelectrics–rejected on elementary considerations of efficiency, materials consumption, and waste heat rejection.
(2) Magnetoplasmadynamics–rejected on grounds of problems in attaining the necessary working fluid temperatures by solar heating.
(3) Direct thermal conversion by electrostatics–insufficient data available for this recently-proposed thermal engine.
(4) Thermophotovoltaics–rejected on consideration of *overall* efficiency and problems of waste heat rejection.

The principal energy conversion conclusions at the completion of Part I were as follows:

(1) Conversion efficiency and resulting SPS size (at fixed output) tended to favor the Brayton gas turbine and gallium arsenide photovoltaic options. A size comparison of the options investigated is shown in Figure 5. Size, however, was not seen as a primary decision factor.
(2) SPS mass was a significant cost factor, especially for hardware that must be delivered to space. Here again, gallium arsenide looked good, with all of the options except thermionics in an acceptable range, as shown in Figure 6. Of the various Rankine cycle working fluids, only the alkali metals were compatible with the high cycle temperatures essential to heat rejection system mass in the acceptable range. (Water, i.e., steam Rankine, is compatible from the fluid thermal stability standpoint, but a steam system operated in the minimum-mass temperature range is essentially a Brayton gas cycle.)
(3) Radiation degradation of solar cells, especially silicon, was known to be a serious problem. The amount of degradation depends on the amount of shielding provided, e.g., by coverglasses. (Attempts to provide lighter weight plastic coverglasses have to date been unsuccessful because the plastics become opaque in the geosynchronous combined radiation and uv environment.)
It has long been known that radiation damage in silicon solar cells can be largely annealed out by heating to ~500°C. This normally would be done by bulk heating. Recent developments had indicated, however, that directed energy pulse heating could be effectively used. As a part of this study, under subcontract, Simulation Physics (now SPIRE, Inc.) conducted exploratory laser and electron beam annealing tests on severely irradiated solar cells provided by Boeing. Approximately 50% of the cells' lost performance was

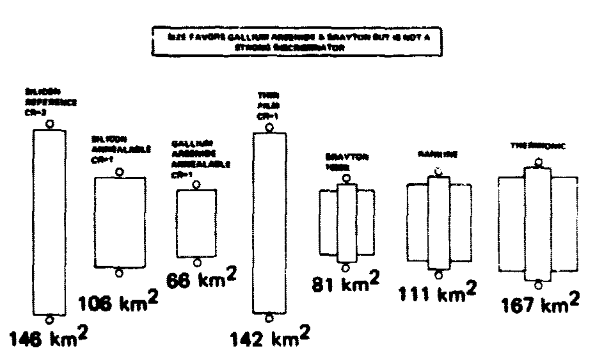

Figure 5. Energy Conversion Comparison SPS Size

ORIGINAL PAGE IS OF POOR QUALITY

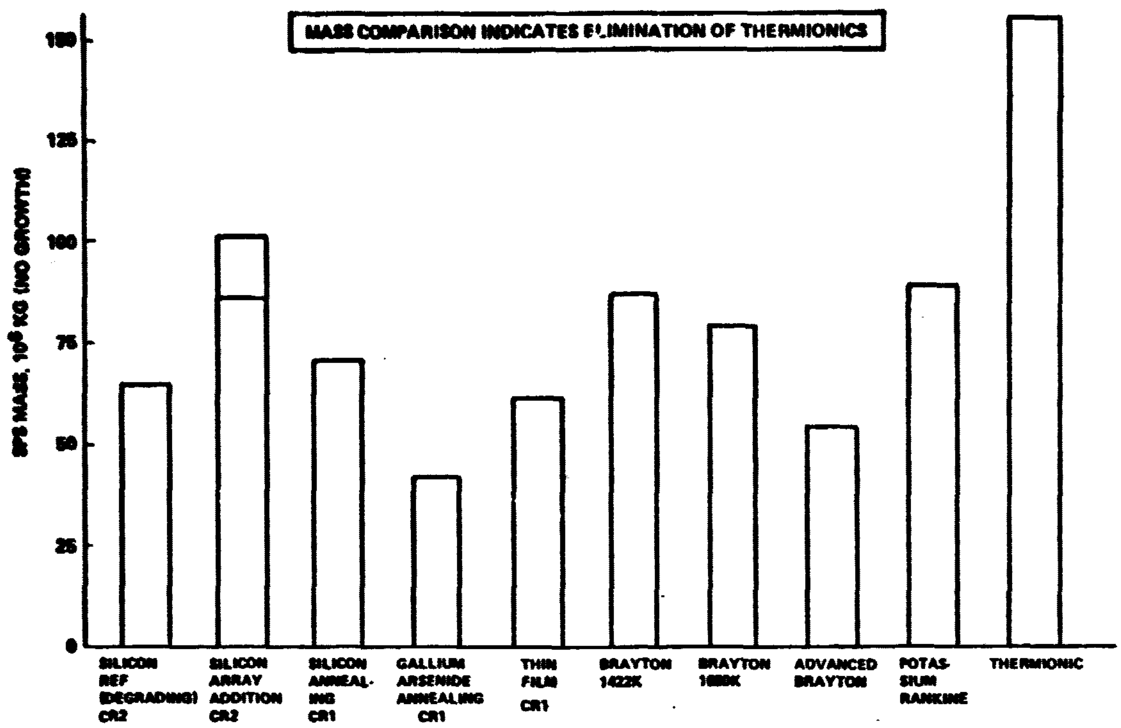

Figure 6. Energy Conversion Comparison SPS Mass

recovered in these tests. It is believed that further development and optimization of the process could approach 90% recovery. Accordingly, an annealable blanket design (compatible with annealing temperature) was selected as the reference design for Part II.

(4) The more complex thermal engine systems were found to be more difficult to construct, but at this point in the study, differences in constructability were not viewed as particularly significant–all configurations were constructable. These differences were later to emerge as a strong decision factor.

(5) If SPS's are to be installed on a large scale, availability of raw materials could be a significant issue. Materials availability was a strong negative factor for the thermionics option. Considered together with excessive mass, the negative factors were judged to be a conclusive reason to discard thermionics. Materials availability also imposed significant design constraints on the other thermal engine options, which benefit from the use of exotic metals at high temperatures. Tungsten, tantalum, and molybdenum were eliminated. Molybdenum itself is not especially scarce, but must be alloyed with rhenium for ductility; rhenium is very scarce. Materials issues were a strong factor in the ultimate selection of potassium Rankine as the preferred thermal engine. This selection, however, did not occur until Part II.

The availability of gallium also emerged as a major issue. This controversy continues to the present day, with gallium arsenide advocates insisting that there is "no problem" and skeptics arguing that the problem is insurmountable. Our evaluation is as follows: *If* thin-film gallium arsenide cells, e.g., on a sapphire substrate, are used with moderate sunlight concentration, and *if* moderately optimistic gallium availability estimates are used, the problem is at least workable, as illustrated in Figure 7. (The cells must be about 5 to 10 μm thick on a substrate of some other material. The physics of gallium arsenide photovoltaics does not preclude such cells being efficient. Gallium arsenide cells presently in experimental production are conventional in thickness, e.g., 100 μm or more.) In view of this issue and the associated technology advancement requirements, this study backed away from gallium arsenide as a primary candidate. It is still so regarded, however, by some investigators. In summary, from the resources standpoint, the silicon system was most favored, thermal engines were readily workable with appropriate design constraints,

and gallium arsenide was probably workable with advanced technology. Some of the other thin-film photovoltaic approaches (e.g., copper indium selenide) were rejected due to resources considerations as was thermionics.

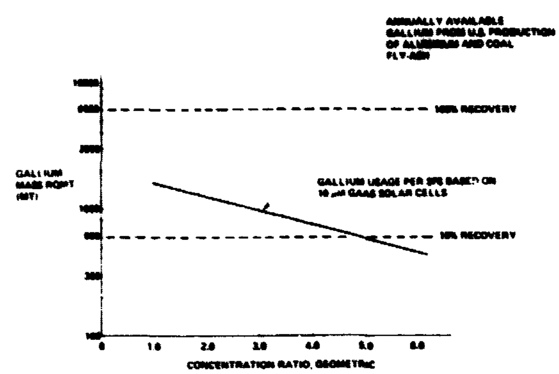

Figure 7. Reduction in Gallium Required for CR>2 System

(6) Technology advancement requirements figured importantly in the eventual selection of preferred systems as well as in the Part I screening stage. A major increase in the scale of space operations must be brought about to install SPS's at a rate of practical interest. Although the technical advancements required in systems and subsystems are quite modest, the required advances in operations technology may be compared to the advances in aircraft operations technology that occurred with the introduction and expansion of the jet age. It is prudent to restrict areas of major technology advance to as few as possible to maximize chances of program success. There was, therefore, a strong motivation to minimize the technological advance required in energy conversion. Silicon photovoltaics and the turbogenerator options fitted this prescription; the other options did not.

(7) Cost and risk are the overriding factors in design selection for any system intended for commercial application. All other parameters are of little significance. (Most of the foregoing factors appear on the cost/risk balance sheets.) At the conclusion of the Part I effort, the silicon photovoltaic and Brayton thermal engine were judged to be essentially equal in cost (Figure 8) and, as noted above, quite comparable in risk. The gallium arsenide option exhibited significant potential cost advantages, mainly resulting from mass and size reductions, but these potentials were heavily overshadowed by the materials availability and technological risk concerns already discussed.

Silicon systems at concentration ratio 1 (i.e., no concentration) and 2 were evaluated. Because concentration is relatively ineffective with silicon due to temperature effects the simpler no-concentration configuration was found to be least cost. Higher solar cell costs improve the benefits of concentration, but these benefits are net positive only when solar cell costs are high enough to make the thermal engine option a relatively uncontested winner. (This conclusion does not necessarily apply to advanced-technology gallium arsenide options.)

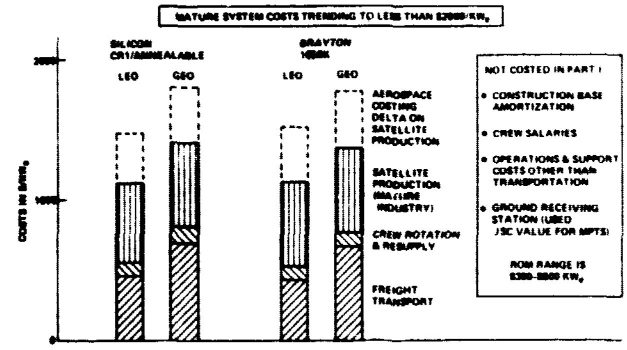

Figure 8. Cost Differential Factors for Reference Systems (Part I Results)

The net result of these considerations was a decision to carry the silicon CR=1 and Brayton energy conversion options into Part II as primary candidates. General Electric, our major subcontractor in this study, expressed the strong opinion that the Brayton-versus-potassium-Rankine tradeoff had not been adequately worked. This matter was re-examined in greater depth as a priority item early in Part II.

Construction Location

The principal construction location conclusions at the end of Part I were as follows:

(1) The primary component of the issue was transportation cost. The payoff for low Earth orbit (LEO) construction is the enabling of the self-powered mode for LEO to geosynchronous Earth orbit (GEO) transportation at the very high specific impulse available through electric propulsion. The propellant requirement for LEO-GEO transportation shrinks from the predominant requirement to a relatively incidental requirement, from 2.1 tons

per ton delivered to GEO to about 0.25 tons per ton. This results in a factor of 2 reduction in launches to low Earth orbit for LEO construction as compared to GEO construction, but poses an array of difficult-to-quantify operational complexities and concerns.

(2) Most important of the negative operational factors associated with the electric propulsion mode are:
   (a) Trip times on the order of six months (compared with less than one day for the high-thrust LO_2/LH_2 systems associated with GEO construction).
   (b) Radiation degradation of the SPS from exposure to the van Allen belts during the slow transfer.
   (c) Modularization of the SPS, necessary for altitude control authority in the presence of the strong gravity gradients at LEO.
   (d) Conversion of the SPS modules into powered spacecraft capable of executing the transfer.
   (e) The risks of collisions with man-made orbiting objects during the LEO construction operations and during the slow spiraling transfer from LEO to GEO.
   (f) Upper atmosphere drag affecting the LEO construction operations.
   (g) Operational hardware and software complexities ensuing from low-thrust orbit transfer operations.

At the conclusion of the Part I effort, the reduction in LEO transportation cost was judged to overwhelm all other factors. The overall reduction in *system* cost was on the order of 10%. The predominant penalty on LEO construction was the added interest cost chargeable to total capital cost as a result of the six month transit times. The investigation of collision hazards was incomplete at this point.

Part II Findings Relative To Part I Issues

The issues addressed during Part I of the study are fundamental and permeate all aspects of system design and selection.

As a result, although narrowing of options, clarification of sub-issues, and focusing of attention was achieved, complete answers were not obtained during Part I. As an example, complete definition of hardware packaging densities and transportation/construction operations options was not achieved until the power transmitter (excluded from Part I) was taken into account.

During Part II, the following major conclusions were obtained relating to the Part I questions:

(1) Continuing comparative evaluation of potassium-vapor Rankine cycle systems versus inert gas Brayton systems led to a preference for the Rankine system because:
   (a) The Rankine system mass-optimizes at somewhat lower mass and much-reduced radiator area.
   (b) The Rankine system is practical, e.g., in terms of hardware mass, at cycle temperature limits generally in the superalloy range, whereas the Brayton systems were dependent on refractory metals or ceramics. Strong implications are present here for technology advancement requirements and resource consumption.
   (c) The Rankine system exhibited good performance at relatively low (circa 30 megawatts) per-engine power ratings. By way of contrast, the Brayton engines are sensitive to blow-by tolerances on turbomachinery and needed to be sized at greater than 300 megawatts per engine. The higher temperatures and power levels required for the Brayton engines have significant cost implications regarding developmental test facilities.

   As a result, and due in no small way to the General Electric subcontract effort, the Rankine potassium vapor cycle was selected as the preferred engine.

(2) Further analyses of transportation and construction operations differences between the thermal engine and photovoltaic options began to reveal significant differences in operations cost. Although differences in satellite mass and cost continued to be unimportant, differences in construction crew size, facility cost, and payload packaging densities emerged as decision drivers as synopsized in Table 1. Consequently, an overall preference for the silicon photovoltaic system gradually became quantifiable. This preference is small, however, with respect to possible uncertainties in solar cell costs, as shown in Figure 9. Therefore, although we recommend the silicon photovoltaic system for preferred concept selection, the Rankine thermal engine should be carried as a backup to hedge against solar cell cost uncertainties.

Table 1. Operations Cost Drivers Favor Photovoltaics

	Silicon Photovoltaic	Rankine Thermal Engine
Construction Crew Size	540	815
Space Construction Base Cost	8.2 Billion	12.4 Billion
Net Packaging Density	95 kg/m^3	65 kg/m^3

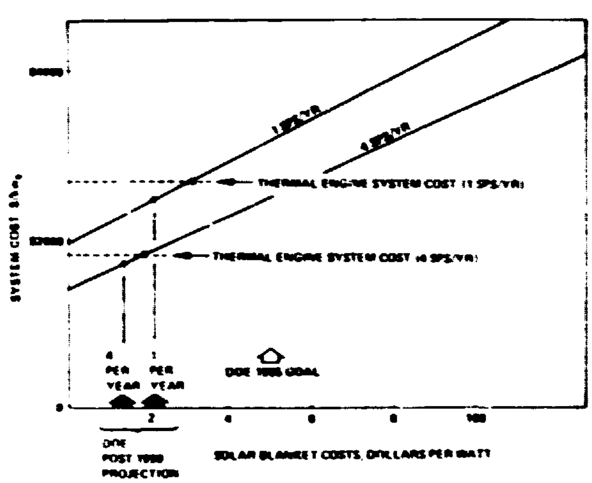

Figure 9. Photovoltaic Preference is Sensitive to Solar Blanket Costs

(3) Construction in low Earth orbit continued to show a ten percent cost advantage. Practical measures were found to avoid collision with any observable man-made objects for which ephemerides are predictable. A refined analysis of system degradation during the 180-day transfer through the van Allen belts revealed no substantive differences from the earlier more parametric analyses. All operational and other LEO/GEO differences were at least roughly quantified and were relatively insignificant in cost. LEO construction offers recurring and nonrecurring cost advantages and is recommended as the preferred concept selection.

MAIN PART II RESULTS

The primary objective of Part II was to accomplish as much system definition as possible within the available study resources. As much reduction as possible in mass and cost uncertainty was the desired outcome of the effort. An economic determination of next program steps can best be made when uncertainties are minimized.

Microwave Power Transmission

The interface requirements and performance of the microwave power transmission system are the keys to an integrated system definition. The performance of the power transmission system establishes overall system sizing and output; the electric power condition requirements of the RF power amplifiers determine the voltages and currents to be produced by the energy conversion system.

The definition effort concentrated on the JSC-originated Klystron option to bring it to the level of definition that had earlier been achieved for the amplitron option.

Figure 10 illustrates the main features of the power transmitter design. The basic power amplifier element is a 70-kw heat-pipe-cooled klystron. Each transmitter element includes one klystron, its control and support circuitry, its thermal control equipment, its distribution waveguides, and its section of radiating waveguide. The subarray is the basic Earth-manufactured unit. It is approximately 10 meters square and employs from 4 to 36 klystron elements. Most of the transmitter electronic complexity is internal to the subarrays. Therefore, completion and checkout of the subarrays on the ground will significantly reduce the workload for space construction and associated hardware/software debugging.

Each 1-km-diameter transmitter includes 6932 subarrays supported on a two-tier structure. At the back of the structure are power processors. These handle the 15% of the electric power fed to the transmitter that requires voltage changes or accurate regulation.

The power transmitter design is largely dictated by constraints. The maximum power intensity in the ionosphere has been limited to 23 mw/cm^{-2}: a best estimate of a limit below which localized ionosphere heating by the power beam will not exceed the heating occasionally produced by natural effects (the fraction of the total ionosphere heated by power beam even from a large number of SPS's is extremely small).

ORIGINAL PAGE IS OF POOR QUALITY

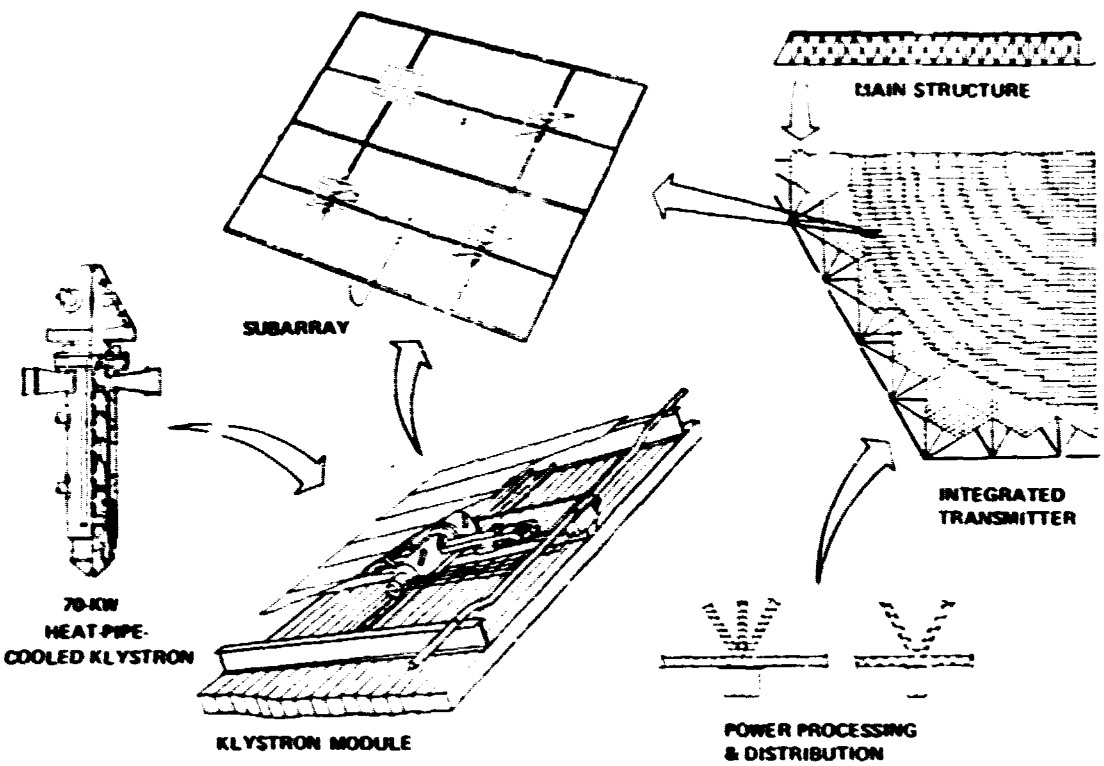

Figure 10. Microwave Power Transmitter Design Concept

It is also desirable to maximize the fraction of total energy within the main beam in order to maximize power transfer efficiency. In addition, minimizing RF energy in beam sidelobes will reduce the microwave energy incident on people as well as other elements of the biosphere (sidelobes are the repetitive low-level maxima in the antenna radiation pattern outside the main beam). Although microwave energy standards applicable to SPS operations have not been set there does not appear to be much doubt that beam-shaping and sidelobe suppression techniques will provide adequate means to control sidelobes as necessary. The simplest beam-shaping technique is tapering of the transmitter power intensity across the aperture as illustrated in Figure 11. Two intensity tapers and resulting beam patterns are shown. The beam pattern intensity scale (db) is a logarithmic scale. Sidelobes 20 db down are 1/100 of the central intensity, 30 db down, 1/1000, etc. Beam shaping capable of reducing sidelobes as much as 45 db was investigated. Figure 12 shows the beam pattern resulting from the 17-db taper option, on a linear scale (sidelobe levels are exaggerated in this plot).

More sophisticated beam-shaping techniques vary the phase as well as the amplitude of the transmitter signal across the aperture. These techniques can "square up" the main beam, providing (a) more total power in a given main beam diameter with a given peak intensity limit, and (b) slightly improved link efficiency. Considerably larger transmitter apertures are required. These techniques will be beneficial to the later phases of an SPS program when very high power per beam is desired.

As the transmitter aperture is increased, the beam diameter at Earth is reduced in inverse proportion. Observing the 23 mw/cm^2 limit, as the beam diameter is reduced, total link power is reduced. As transmitter aperture is decreased, allowing increased link power, a thermal limit is reached due to increasing intensity of waste heat dissipation on the antenna. If the desired link power does not require operating at the 23 mw/cm^2 limit, the transmitter aperture may be cost-optimized. The effect of these limits is shown in Figure 13. (This result assumes the peak *sidelobe* intensity to be constrained to no greater than 0.01 mw/cm^2. Changing the sidelobe constraints influ-

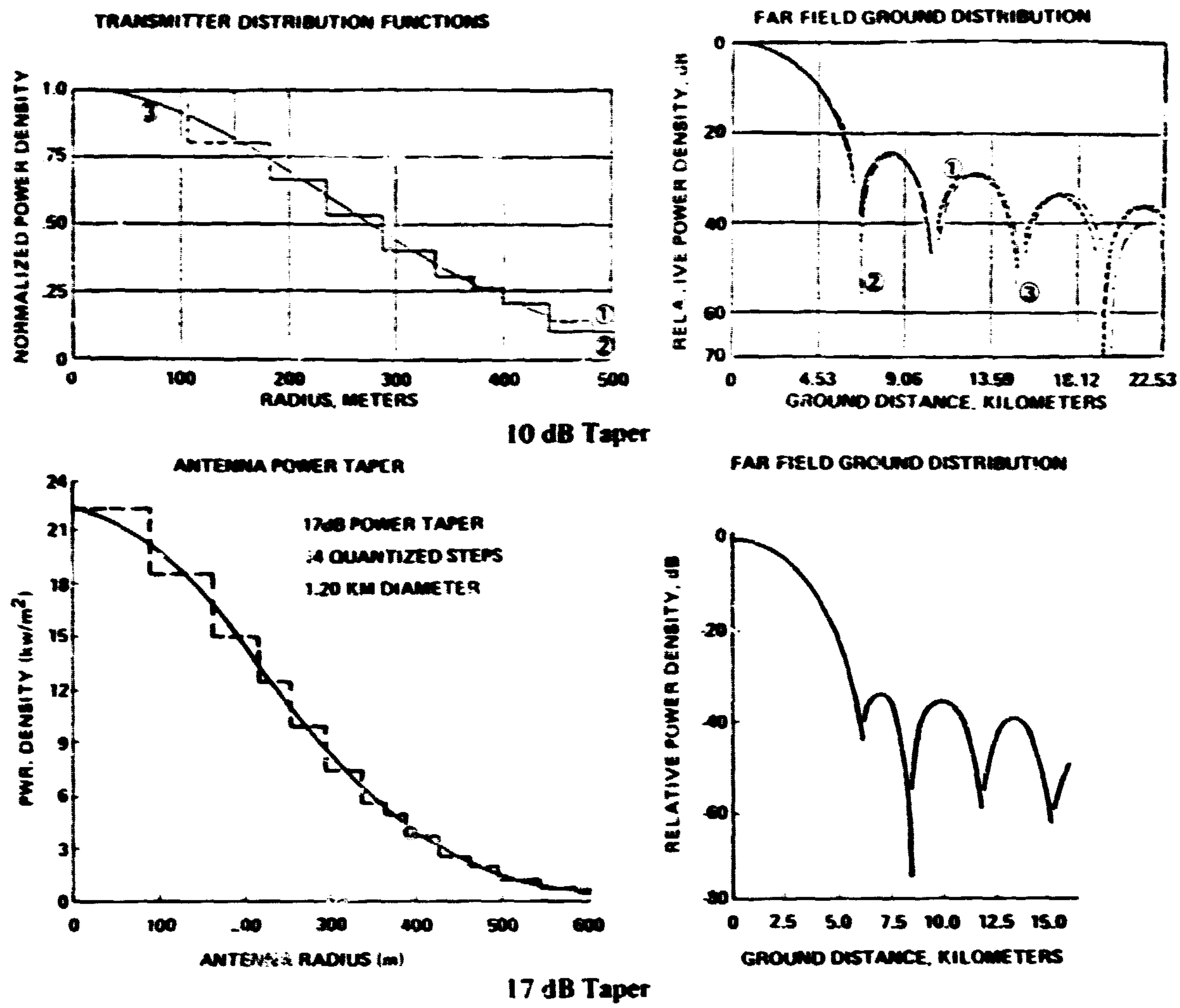

Figure 11. MPTS Power Density Taper

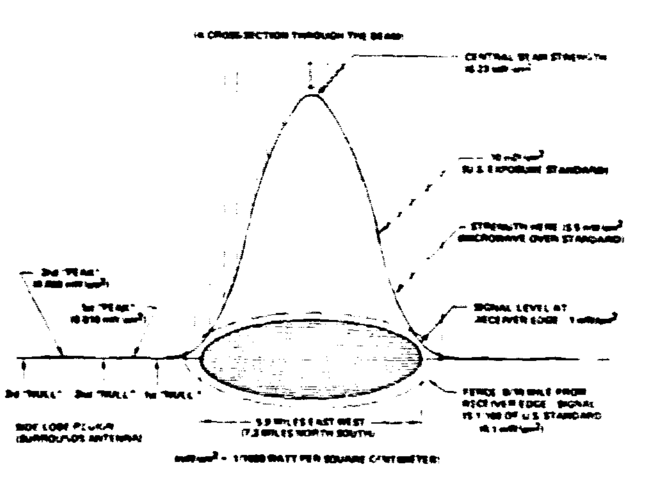

Figure 12. Microwave Beam Intensity on a Linear Scale

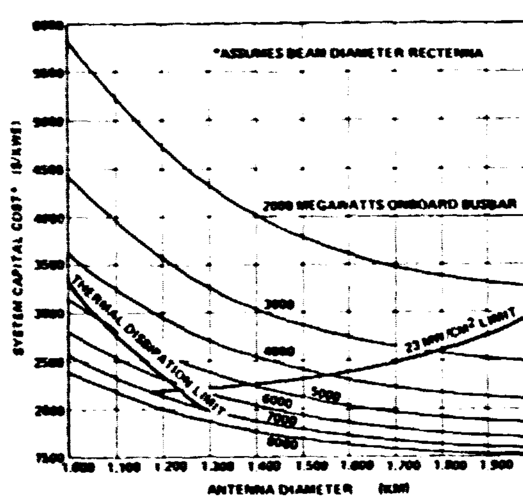

Figure 13. Transmitter Constraints Determine Minimum Cost Design Point

ences the thermal limits: higher permitted sidelobe limits thereby allow smaller transmitter apertures and greater link power.) The most cost effective system operates at the point where thermal limits and main beam intensity limits intersect.

Additional design constraints influence details of the transmitter design and were taken into account in selecting the reference and alternate design points. They are discussed in more detail in Volume 4 of this report. Table 2 summarizes the main features of the power transmission system design. Current values are compared with the values from the JSC "green book" (JSC-11568) with reasons for changes noted.

Table 2. Power Transmission System Highlights

	JSC GREEN BOOK	CURRENT REFERENCE	REASON FOR CHANGE
OUTPUT POWER TO GRID FROM EACH RECTENNA	[illegible]	[illegible]	EFFICIENCY CHAIN VARIANCE
ARRAY APERTURE ILLUMINATION	10-STEP TRUNCATED 10-dB GAUSSIAN	SAME	
ALTERNATE ILLUMINATION		10 STEP 17 dB	PROVIDES ADDITIONAL 10dB OF SIDELOBE SUPPRESSION
SUBARRAY SIZE	[illegible]	[illegible]	GEOMETRIC CONSTRAINTS
NUMBER OF SUBARRAYS	[illegible]	[illegible]	LARGER AREA PER SUBARRAY
ERROR BUDGET			
PHASE CONTROL	[illegible]	SAME	
AMPLITUDE	1dB	SAME	
SUBARRAY MECHANICAL	3 ARC MIN	1 ARC MIN	REDUCE LOSSES
RF DISTRIBUTION	NONE	2% TOTAL LOSS	DETAILED SUBARRAY ANALYSIS
PHASE CONTROL	ACTIVE RETRO DIRECTIVE	SAME	
RECTENNA SIZE	10 x 13km	[illegible] x 13 km	HIGHER RECTENNA UNIT COSTS YIELD SMALLER OPTIMUM SIZE
MAXIMUM BEAM POWER DENSITY	23 mw/cm^2	SAME	

Additional significant results of the microwave system definition effort were:

(1) A detailed analysis was made of the efficiency achievable by microwave power transmission. Table 3 compares the results with the values from the JSC "green book" (the photovoltaic reference efficiency chain is included). The principal new factor is the intra-subarray effects resulting from manufacturing tolerances on subarray hardware. Limiting these losses to 2% requires high-precision manufacturing. This again underscores the desirability of completing the subarrays on the ground.

(2) Investigations of phase control techniques concentrated on the retrodirective technique. This technique employs a signal transmitted from the ground receiving antenna to implicitly measure, and correct for, mechanical inaccuracies in the transmitting antenna. Desirable power transmission system efficiencies require the wavefront emitted from 1-km-diameter transmitter to be planar within ±3 mm (±10° phase error). Mechanical perfection of this degree is difficult to imagine, but the phase front can be electronically controlled to be

Table 3. Nominal Efficiency Chains —Photovoltaic SPS

ITEM	JSC GREEN BOOK	CURRENT NOMINAL	REASON FOR DIFFERENCE
SUMMER SOLSTICE FACTOR	NOT INCLUDED	[illegible]	THESE WERE INCLUDED IN ENERGY INTENSITY ON SPS
ORBIT LOSS [illegible]	NOT INCLUDED	[illegible]	
SOLAR CELL EFFICIENCY		[illegible]	
RADIATION DEGRADATION		97	
TEMPERATURE DEGRADATION	[illegible]	[illegible] [illegible]	SLIGHTLY BETTER CELL, CR = 1
COVER UV DEGRADATION		[illegible]	
CELL TO-CELL MISMATCH		[illegible]	
PANEL LOST AREA	NOT INCLUDED	[illegible]	
STRING I^2R	[illegible]	[illegible] [illegible]	DISTRIBUTION OPTIMIZATION
BUS I^2R		[illegible]	
ROTARY JOINT	1.0	1.0	
ANTENNA POWER DISTR	[illegible]	97	PROCESSING & TEMPERATURE VARIANCE ESTIMATE
DC RF CONVERSION	[illegible]	[illegible]	
WAVEGUIDE I^2R	[illegible]		
IDEAL BEAM		[illegible]	
INTER SUBARRAY ERRORS	[illegible]	[illegible] [illegible]	INTRA SUBARRAY EFFECTS NOT INCLUDED IN GREEN BOOK
INTRA SUBARRAY ERRORS		[illegible]	
ATMOSPHERE ABSORP	[illegible]	[illegible]	
INTERCEPT EFFICIENCY		[illegible]	
RECTENNA RF DC	[illegible]	[illegible]	NUMERICAL INTEGRATION
GRID INTERFACING	[illegible]	97	INCLUDES DC DC PROCESSORS
PRODUCT SIZES (km^2)	[illegible]	[illegible]	

far more precise than the mechanical alignment of the antenna. This can be accomplished by distributing a reference phase synchronization signal to all subarrays from a common source on the antenna and comparing this signal with the signal transmitted from the ground. Phase integrity of the onboard reference distribution system depends on accurate measurement of the path lengths over which the signal is distributed. Explicit and implicit measurement methods were identified. The explicit means was selected as the reference design, but either method would work.

There are some doubts as to whether the retrodirective scheme can provide a sufficiently precise reference to establish an accurate transmitted wavefront. Self-contained onboard methods are possible. Experimental exploration of the phase control alternatives is urgently needed and is one of the top-priority SPS technology verification needs.

(3) Active thermal control was found to be necessary for the antenna power processors. This is because (a) the processors need to be sized at several megawatts to be lightweight and efficient and (b) they need to be cooled to about 50°C; (c) the resulting radiator size per processor is too large to be effectively served by heat pipes. Heat pipe cooling of the klystrons is practical; entirely analogous heat pipe applications have been developed, e.g., by Hughes Electron Dynamics Division.

(4) Rectenna costs were found to be a major factor in overall power transmission system costs. The rectenna cost per unit area also figures strongly in system cost optimization.

Table 4 summarizes typical rectenna characteristics. Main cost drivers are primary and secondary structure at an estimated \$13/m^2 and the dipole/diode/filter units at an estimated \$ /m^2, resulting in a total cost of about \$2.2 billion. Due to the shape of the beam intensity patterns, cost savings due to reduction in rectenna size can be effectively traded for power lost as shown in Figure 14. The outer regions of the main beam contain relatively little energy; it costs more to collect than it is worth. Typically, the cost optimum rectenna diameter is 70 to 75% of the main beam diameter. The optimal rectenna intercepts about 95% of the energy in the main beam.

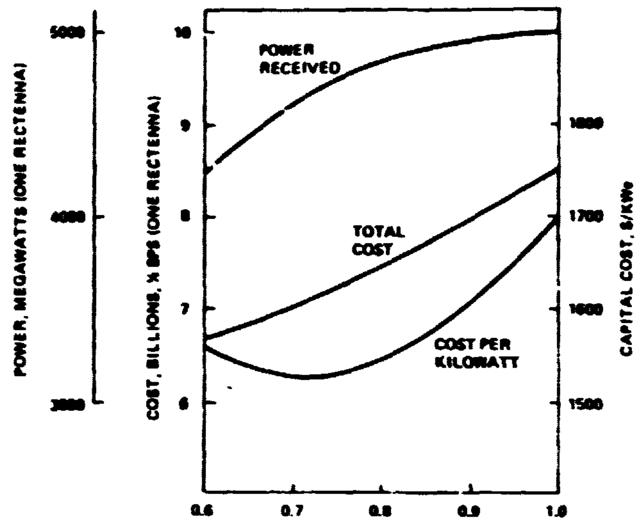

Figure 14. Rectenna Size Optimization

Table 4. Rectenna Nominal Cost Estimate @ 1 SPS/YR

BEAM DIAMETER	13 KM
RECTENNA INTERCEPT DIAMETER	9.36 KM @ 93% EFFICIENCY
RECTENNA GROUND AREA	= $1.536 \times \pi/4 \times 9.75^2 = 165$ KM^2
RECTENNA PANEL AREA	= 68.8 KM^2
TOTAL CONTROLLED AREA (LAND ACQUIS)	= 204 KM^2 = 50,400 ACRES

SPS Configurations

The photovoltaic reference configuration is a simple two-level planar structure supporting approximately 102 km^2 of solar arrays, as illustrated in Figure 15. The solar blanket is divided into 256 bays each 660 meters square. The SPS consists of eight modules each four by eight bays, and the two rotary joints, yokes, and transmitters. Modularization facilitates self-powered orbit transfer; a satellite constructed at geosynchronous orbit could be monolithic in design with about 1 120 000 kg less total structural mass. Table 5 provides additional design highlights.

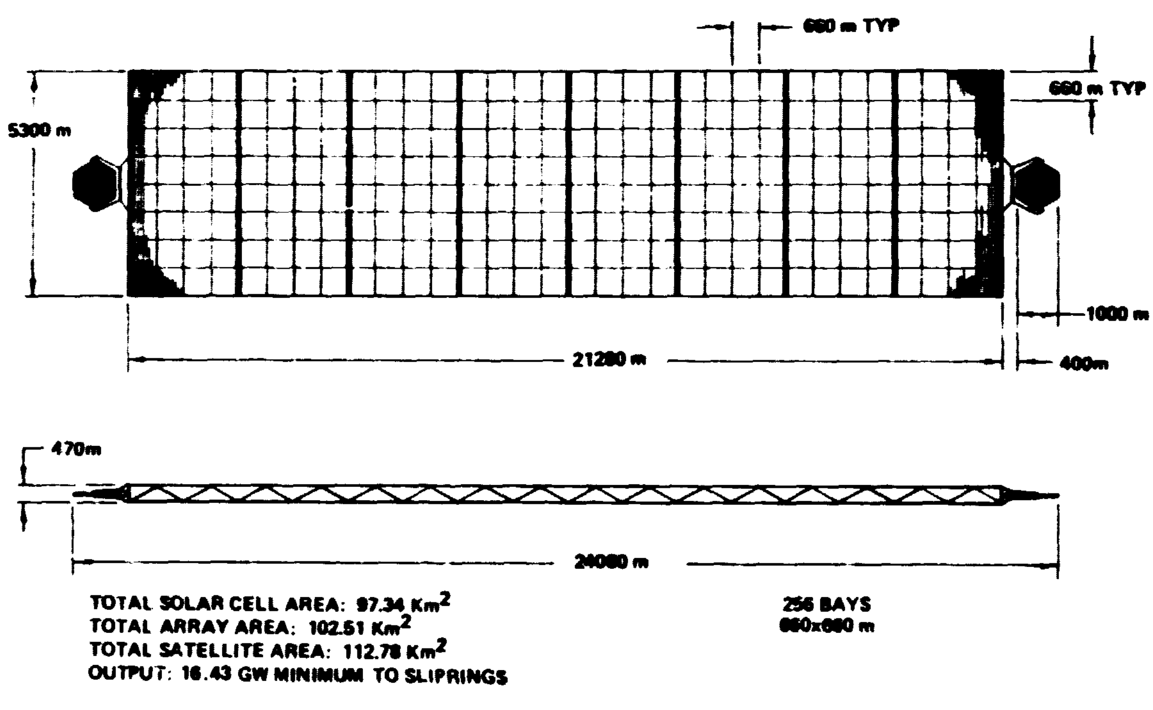

Figure 15. Photovoltaic Reference Configuration

Table 5. Photovoltaic System Highlights

SOLAR CELL EFFICIENCY	17.3% (15.8% CELL WITH SAW-TOOTH COVER)
SOLAR CELL THICKNESS	50 μm
COVER THICKNESS	75 μm
SUBSTRATE THICKNESS	50 μm
BLANKET UNIT MASS	0.427 kg/m^2
CELL AREA	97.3 km^2
BLANKET AREA	102.5 km^2
OVERALL AREA	112.[illegible] km^2
SOLAR BLANKET COST	$35/m^2
STRUCTURE COST	[illegible]/kg
FLIGHT MODE	PERPENDICULAR TO ORBIT PLANE WITH ELECTRIC THRUST
POWER DISTRIBUTION	40 KV WITH 208 ISOLATABLE POWER SECTORS. PASSIVELY-COOLED-DEDICATED-ALUMINUM SHEET CONDUCTORS
POWER MAINTENANCE	PERIODIC ANNEALING

The basic manufactured unit shown in Figure 16 is a solar blanket panel approximately one meter square containing 252 solar cells (18 in series by 14 in parallel). The 50 μm solar cells are more radiation resistant than thicker cells considered earlier in the study. It is estimated that these blankets will require annealing 6 to 10 times in a 30-year period.

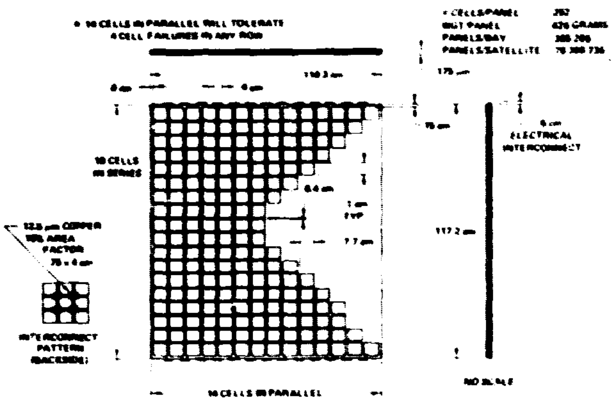

Figure 16. Photovoltaic Reference Configuration Solar Array Fundamental Element "Blanket Panel"

The blanket panels are assembled into installable blanket packages by welding the interpanel connectors and taping the panels together. The installable packages are 20 m wide by one bay length (660 m) long, and are shipped accordion-folded in a suitable box. Blanket packages are joined together edge-to-edge (electrical connection not required) on installation, so that each bay of solar blanket becomes like a large trampoline as shown in Figure 17. Stretch loads are carried by the tape grid, and are applied through a catenary support that attaches to structural hardpoints at a 20-meter spacing. The load at each attach point is 90 newtons; this provides a blanket "trampoline" frequency of about 12 cycles/hr, higher than the first few SPS structural modes.

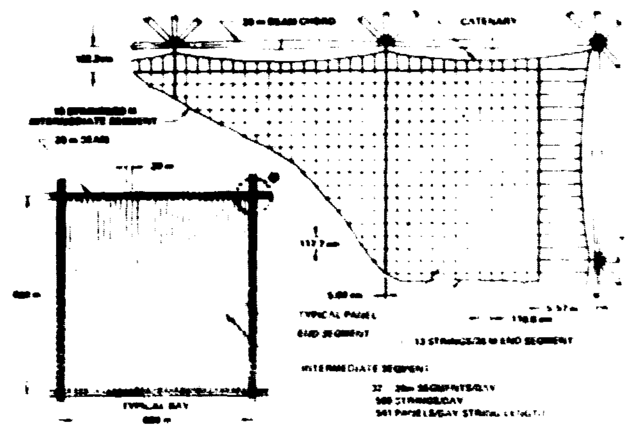

Figure 17. Photovoltaic Reference Solar Array Arrangement and Attachment

Minimum-mass structural configurations employ closed-section members of extremely low packaging density. Two approaches to reaching acceptable densities have been developed:

(1) Fabricate the structural members in orbit, using "beam machines" that thermally form specially-prepared flat stock shipped to orbit in rolls; after thermal forming, ultrasonic welding or other bonding techniques are employed to assemble the structural beams.

(2) Use an element configuration that permits nesting at acceptable densities for shipment. The "beam machines," in this case, assemble the beams from these prefabricated parts, using prefabricated mechanical joints of suitable design.

No clear conclusion was reached as to which of these approaches is best. Additional technology verification work is needed to accomplish a selection.

For power management and power distribution, the photovoltaic SPS is divided into 208 power sectors. Each power sector is switchable and can be isolated from the main power bus, facilitating annealing or other servicing. Main features of the power distribution system are shown in Figure 18. Power transfer across the rotary joint is accomplished by a slip ring/brush assembly. The size of this assembly, 16 m in diameter, is such that it can be completed and checked out on the ground. Mechanical rotation and drive is provided by a mechanical turntable 150 m in diameter. The antenna is suspended in the yoke by a soft mechanical joint to isolate the antenna from turntable vibrations. The antenna is mechanically aimed by CMG's installed on its structure. A position feedback with a low frequency passband allows the mechanical turntable to drive the yoke to follow the antenna and also provide sufficient torque

through the soft joint to keep the CMG's desaturated.

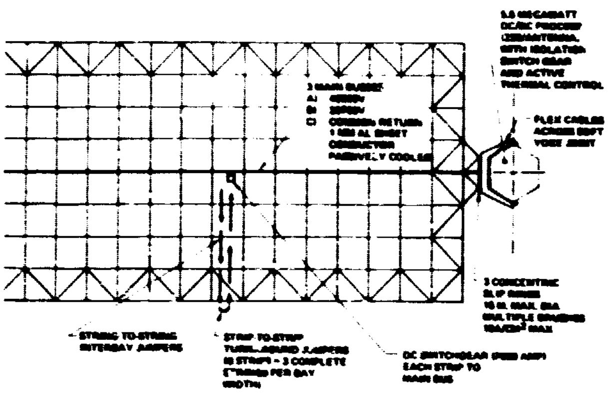

Figure 18. SPS Power Distribution is Straightforward Engineering

The overall efficiency chain for the photovoltaic SPS was compared with the point-of-departure (JSC "green book") figures in Table 3. Principal changes occurred with the change to concentration ratio 1 and with a detailed efficiency analysis for the power transmission system. The photovoltaic mass estimate history has remained relatively consistent, as shown in Figure 19. The current mass estimate is summarized in Table 6, compared with the original JSC "green book" estimates.

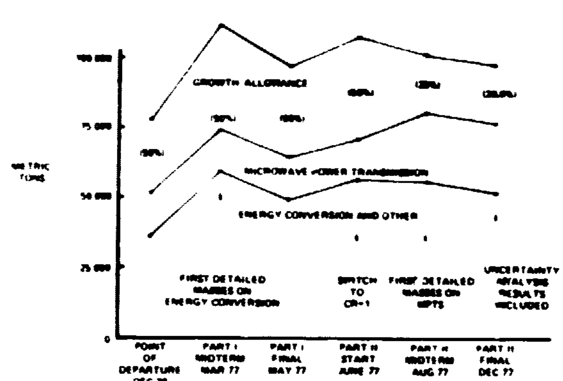

Figure 19. Reference Photovoltaic SPS Mass Estimate History

As the Part II effort began, the final question of choice between potassium vapor Rankine and inert gas Brayton power generation for the preferred thermal system was still open. The Part I effort had concentrated on trying to closely match the Brayton thermal cycle efficiency (~40%) with the Rankine system. Further analyses indicated clearly that basic differences in the cycles and their types of machinery caused this efficiency matching to show the Rankine option in a bad light. At a

Table 6. Silicon Photovoltaic Mass Properties Summary

ITEM	JSC "GREEN BOOK" MASS	CURRENT MASS	REASON FOR CHANGE
MULTIPLE/COMMON USE EQUIPMENT	(3467)	(5636)	
PRIMARY STRUCTURE	2973	[illegible]	• DESIGN LOADS
OTHER	[illegible]	[illegible]	
ENERGY COLLECTION	(5736)	(0)	• CHANGE TO CR = 1
ENERGY CONVERSION (SOLAR BLANKETS)	(20677)	(43750)	• CHANGE TO CR = 1 • GLASS CELL COVERS
POWER DISTRIBUTION	[illegible]	(2300)	
POWER TRANSMISSION	(15371)	(25212)	
STRUCTURE	1210	[illegible]	• SUBARRAY STRUCTURE IN SUBARRAYS
POWER DISTR	[illegible]	[illegible]	• PROCESSORS & THERMAL CONTROL
MICROWAVE GENERATORS	[illegible]	[illegible]	• THERMAL CONTROL
SUBARRAY STR & WAVEGUIDES	[illegible]	4314	
CONTROL ELEX	[illegible]	970	
OTHER	[illegible]	72	• GREEN BOOK CARRIED ROTARY JOINT IN ANTENNA MASS
SUBTOTAL	[illegible]	[illegible]	• DETAILED UNCERTAINTY ANALYSIS
GROWTH	(50%) [illegible]	(26.0%) [illegible]	
TOTAL	[illegible]	[illegible]	

given cycle peak temperature, as the radiator mean temperature is lowered, the Brayton machinery mass decreases and the radiator mass increases. The optimum is reached at cycle efficiencies in the vicinity of 40%. The Rankine hardware, however, becomes quite massive at lower radiator temperatures and the system optimizes at much lower efficiencies, on the order of 20%. The result of these analyses was that the optimized Rankine system was indicated to be less massive than the Brayton system in the cycle temperature ranges of main interest (at very high cycle peak temperatures and accordingly very advanced materials, the Brayton system is least massive).

Further analyses of materials availability and newer data on long-term creep characteristics indicated that cycle peak temperatures should be reduced from about 1600K to about 1250K. This tended to penalize the Brayton system but provided a nearly ideal match to the fluid properties of potassium.

Simplicity was a further consideration. The Rankine cycle system is less complex than the Brayton system as is illustrated in Figure 20. All these considerations led to a switch to a potassium Rankine reference system design. An additional simplification was introduced by selecting a perpendicular-to-ecliptic plane (PEP) orientation. With the satellite attitude controlled to be exactly sun-facing within one degree, and the addition of a second-stage concentrator at the focal point assembly, the need for steerable facets was eliminated. The resulting configuration is shown in Figure 21. Sixteen modules are arranged in a square pattern with antennas at two of the corners. This arrangement provides adequate antenna beam clearance

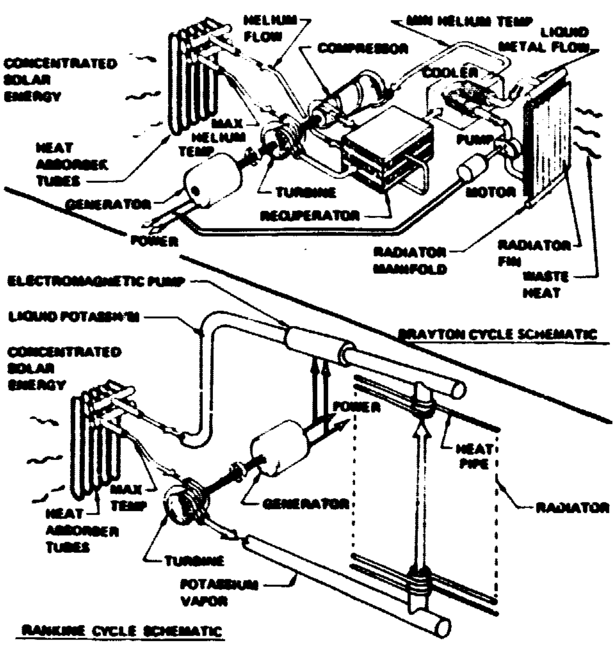

Figure 20. Brayton and Rankine Cycle Flow Schematics

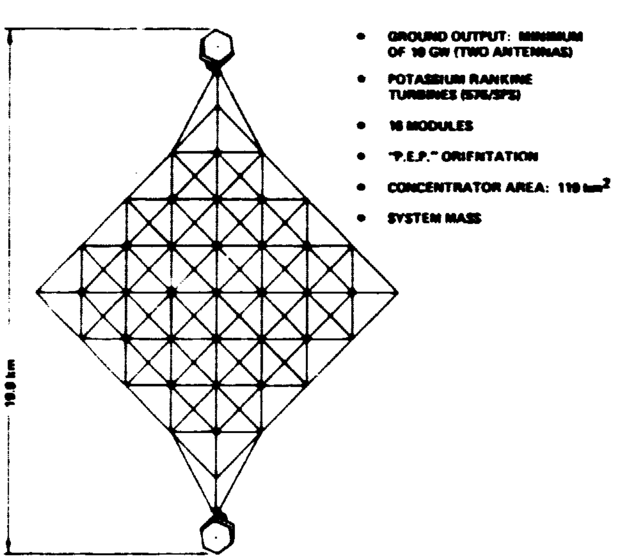

Figure 21. Reference Rankine SPS Design

with the PEP orientation at all times of year. Figures 22 and 23 show further details of the focal point assembly and turbogenerator pallet arrangement. The PEP orientation requires considerably more attitude control propellant (about 150 tons/year compared to 40 tons/year) than the perpendicular-to-orbit-plane (POP) orientation used for the photovoltaic system. The advantages of PEP operation with the thermal engine are sufficient to justify the additional expenditure; this is not true for the photovoltaic system. One disadvantage of PEP operation is the requirement for the two-axis rotary joint shown in Figure 21. The additional axis is needed to maintain correct polarization of the transmitter with respect to its ground station.

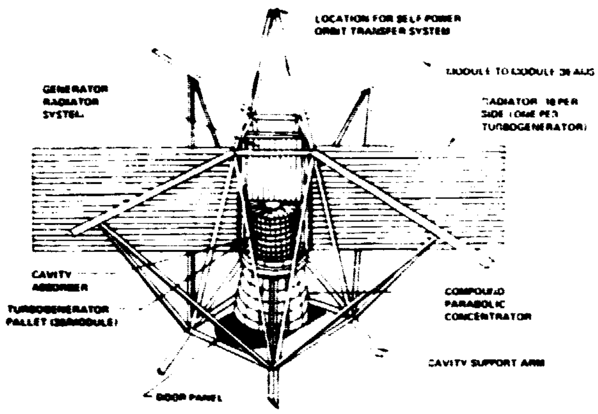

Figure 22. Focal Point Assembly

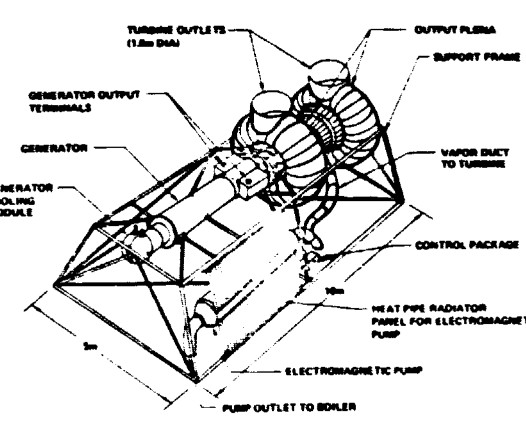

Figure 23. Turbogenerator Pallet

During Part II new information was obtained on plastic film reflector degradation in the space radiation environment. Tests conducted on the JPL solar sail effort indicated that no degradation of reflective surfaces would occur. Boeing IR&D radiation chamber tests currently in process are confirming this result. Accordingly, the concentrator was reduced in size from the earlier designs that provided 30% concentration oversize to compensate for radiation degradation of reflectivity.

The thermal engine efficiency chain is shown in Table 7. The overall energy conversion efficiency for the thermal and photovoltaic options is virtually the same: both use the same power transmission system.

Table 7. Comparison of Efficiency Chains

RANKINE THERMAL ENGINE

ITEM	NOMINAL	MINIMUM	MAXIMUM
CONCENTRATOR	.877	.83	.96
REFLECT DEGR	1.0	.70	1.0
CPC	.965	.90	.985
CAVITY OPTICAL	.960	.95	.98
CAVITY RERADIATION	.917	.917	.934
CAVITY THERMAL	.995	.990	.997
CYCLE	.189	.189	.200
GENERATOR	.984	.984	.986
PARASITIC	.962	.944	.98
POWER DISTR	.948	.93	.96
MPTS (FROM P/V)	.563	.412	.683
PRODUCTS SIZES	.0628 118 KM^2	.027 274 KM^2	.085 77.8 KM^2

The thermal engine mass estimate history has exhibited somewhat more variation than the photovoltaic system. This has been largely due to the greater system complexity and to changes in cycles and cycle temperatures. The current thermal engine mass statement is given in Table 8.

Table 8. Potassium Rankine SPS Mass Statement

	10^6 kg
STRUCTURE	6.976
FACETS	1.837
RADIATOR (W/O POTASSIUM)	10.768
POW DIST	4.760
SW. GEAR	0.218
GENERATORS, ACCESSORY PACK	2.508
GENERATOR RADIATORS	1.140
TURBINES	13.755
PUMPS, PUMP RADIATORS	0.984
BOILERS & MANIFOLDS	3.296
CAVITY ASSYS	1.000
CPCS	0.299
LIGHT DOORS	0.025
MONITOR, COMMAND & CONTROL	0.100
ATTITUDE CONTROL	1.200
START LOOPS, CONTROLS	0.250
ANTENNA SUPPORT	0.286
MISC, INCLUDING STORAGE	0.200
POTASSIUM INVENTORY	6.058
POWER GENERATION	55.660
ANTENNAS	24.384
SPS	80.044

An overall preference for the photovoltaic system emerged late in the study due to better quantification of operations cost penalties associated with thermal engine system complexity. This preference is, however, somewhat sensitive to solar blanket costs and depends on achievement of low costs at high production rates.

Construction Systems

The most novel problem presented in developing an overall SPS systems definition was to evolve a conceptual design of a construction facility capable of constructing a 100 square-kilometer object in orbit. Earlier SPS studies gave little attention to SPS construction. Issues such as microwave power transmission, space transportation, and feasible lightweight designs for the enormous SPS structures seemed more crucial. Some of the SPS concepts were either too ill-defined or in such a fluid state that an adequate construction analysis was not possible. Construction analyses must be conducted at a detail level; high-level parametrics tend to be meaningless.

The other issues appeared more resolvable by the beginning of this study. Increased attention was turned to the formidable and largely unexplored problem of construction of SPS's in space. We were faced with four challenges:

- No one had ever designed or built anything like an SPS structure, or any contiguous self-supporting structure remotely approaching the size of an SPS. (The solar collector area of a 10,000 megawatt SPS is greater than the surface area of Manhattan Island.)
- No one had ever designed or built a large structure for loads criteria anything like as low as those applicable to an SPS. (We have used 0.0001 g as a preliminary criterion. Conventional spacecraft have, of course, been designed for launch loads in the range from 5 to 10 g's.)
- No one had ever designed a factory or any construction equipment to operate in hard vacuum at near-zero g.
- Initial studies of SPS construction quickly scoped space crew productivity requirements. Construction of one 10,000 megawatt SPS in one year could afford to employ some hundreds of people working in space. Roughly 10^6 construction manhours (expended in space) could be used. This represents a productivity factor on the order of 10 manhours/ton, about equivalent to that for steel high-rise construction. If, for example, a productivity factor like that for jet aircraft assembly

(about 2000 manhours/ton) were experienced, the costs to support space construction activities would exceed economically feasible SPS costs.

Some of the earliest concepts of SPS construction imagined crews in space suits assembling SPS's with hand tools. These early views recognized neither the size of SPS hardware nor the crew productivity rates required.

Several high-level ground rules were adopted at the beginning of the current effort.

- **Facilitized Construction**: Satellite design is not penalized by construction equipment support requirements.
- **Decoupled Operations**: Construction operations should be independent as possible so that a slowdown or shutdown in one operation has minimum impact on others.
- **Operations in Parallel**: Fabrication operations in parallel in separate facility locations so that maximum time can be allotted to each type of operation.
- **Moving Beam Machines**: Number of machines determined by output rate rather than numbers of parallel beams in the SPS. This maximizes effective use of expensive equipment.
- **Support the Beams**: Long beams should be supported as they are fabricated to eliminate undesired stress and unguided end positions.
- **Minimize Use of Free Flyers**: The satellite components are too frangible to tolerate accidental collisions. Propellant consumption, exhaust product contamination, and plume impingement would present problems.

The photovoltaic construction facility that evolved over the period of the study is shown in Figures 24 and 25. The first of these shows the overall arrangement; the second is an artist's concept of a portion of the facility and gives a better impression of the lightweight structural design that would be applied to the facility as well as the SPS.

The facility is a combined power transmitter antenna and photovoltaic energy conversion construction facility. It is mainly a C-clamp-shaped truss structure. In Figure 24, the structure is shown boxed in for most of the facility to clarify the illustration but would actually appear as indicated by the "actual structure" callout. Overall facility dimensions are 1.4 x 2.8 km. Crew modules and launch vehicle docking stations are shown approximately to scale.

The crew modules are sized for 100 people (17 meters diameter by 23 meters length). The facility includes 4 bays dedicated to structure

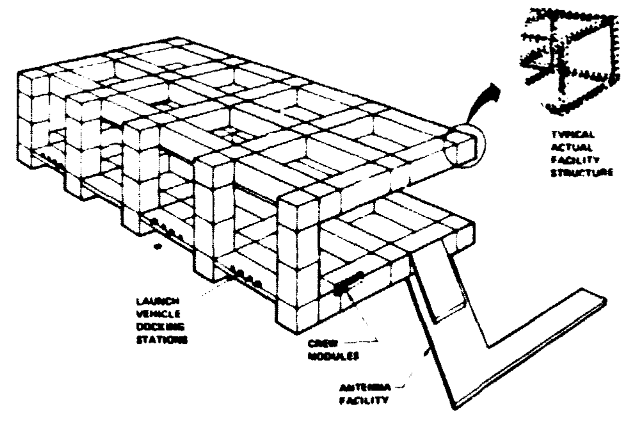

Figure 24. Photovoltaic Construction Facility Arrangement

manufacture and 4 bays dedicated to solar blanket and equipment installation.

The construction base concepts (thermal engine construction bases were also defined) evolved gradually over the entire period of the study. The analysis procedure was conducted in a "grass roots" fashion, beginning with concepts for construction machines to perform specific tasks, and proceeding through machine production rate estimates, task manloading and timelining, and finally building up to the base definition level. By far the majority of the effort was invested in defining the facility and equipment. The crew habitats were only externally defined (mass, size, crew capacity) based on extrapolations from earlier and concurrent space station studies. The crew habitats, however, represent a major proportion of total base cost.

Highlight statistics for the construction bases are given in Table 9. Although the crew sizes and construction base masses and costs seem quite large by traditional experience, construction operations costs (including crew transportation and amortization of the bases) only contributes about 8% of the total SPS capital cost.

Table 9. Construction Highlights

	PHOTOVOLTAIC LEO CONSTRUCTION	PHOTOVOLTAIC GEO CONSTRUCTION	THERMAL LEO CONSTRUCTION	THERMAL GEO CONSTRUCTION
• CREW SIZE	560	[illegible]	815	835
AT LEO	480	70	760	105
AT GEO	80	480	55	730
• CONST START TO ON LINE TIME FOR 1 SPS	[illegible] DAYS	354 DAYS	575 DAYS	[illegible] DAYS
• CREW WORK SCHEDULE	10 HOURS/DAY 6 DAYS/WEEK 2 SHIFTS			
• CREW STAYTIME	30 DAYS	[illegible] DAYS	90 DAYS	90 DAYS
• MAIN BASE SIZE	2.8 x 1.0 x 1.0 km		3.5 x 3.2 x 2.8 km	
• BASE MASS (METRIC TONS)				
AT LEO	5870	780	9000	1100
AT GEO	770	6535	880	10040
• BASE COST (LEO & GEO)	8.7 BILLION		12.4 BILLION	
• HLLV LAUNCHES TO DELIVER BASE	61	93	95	144

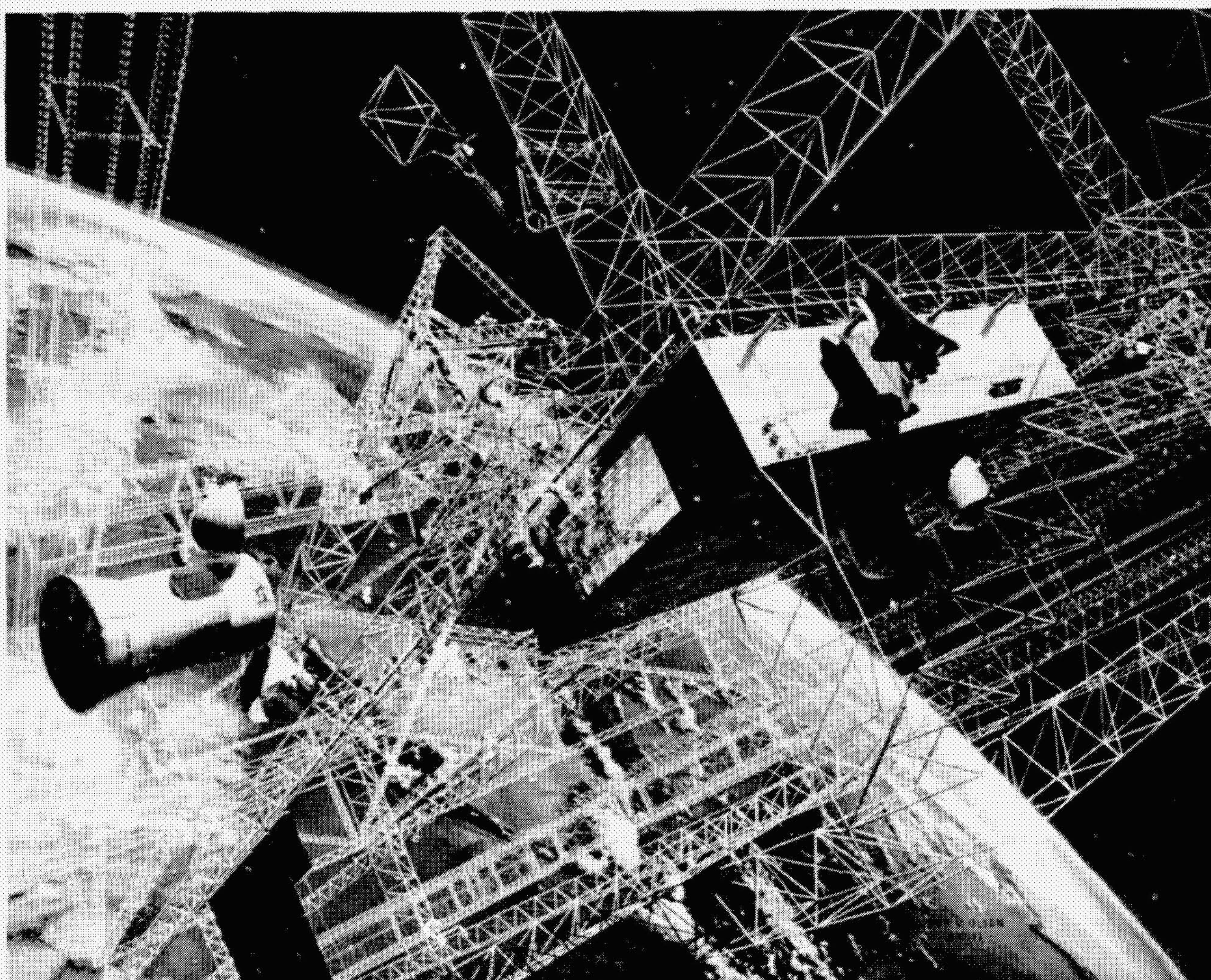

Figure 25. Construction Facility Concept

Significant conclusions from the construction analysis were:

(1) Base and equipment costs are significant; effective utilization is essential. This is, of course, true for Earth-based manufacturing plants.

(2) The required construction rate determines the desirable base size and quantity. Construction bases were sized for 1 SPS per year. Effective base utilization requires continuous operations; the achievable production rate should not exceed the SPS installation rate.

(3) Large launch vehicle payload volume will reduce construction base transportation costs. The estimated base hardware packaging density is about 40% of that for SPS hardware.

(4) The facility design has evolved to an assembly line concept that maximizes crew and machine productivity and minimizes satellite design problems.

(5) The crew are primarily machine supervisors. Little need for EVA has been identified.

(6) Construction base onboard logistics is an important design factor. The SPS hardware throughput is 15 tons per hour for a construction rate of one SPS per year. To maximize packaging density, hardware types have been mixed, e.g., solar cells and transmitter subarrays may go on the same launch. Payload unpacking and distribution to the operating construction machines is a significant part of the total effort.

Transportation Systems

The need for the equivalent of 1000 or more Saturn V launches to deliver one SPS to its operational orbit has been used to "prove" the practical infeasibility of the SPS concept. Certainly at Saturn V costs, the cost of transportation alone would be at least ten times what one could reasonably expect as an economically feasible cost for an SPS. This argumement is, of course, invalid. The Saturn V design stemmed from a technology base now about two decades old. Concepts for vehicle reusability were available at that time but were considered as unnecessary contributors to development risk in view of (a) the urgency of the Apollo program, and (b) the comparatively few launches that were planned.

SPS transportation studies have developed vehicle design concepts responsive to the high launch rate requirements of an SPS program. These concepts have included fully reusable ballistic or winged Earth launch vehicles, and reusable orbit transfer systems for transportation from Earth's surface to low Earth orbit (LEO) and between LEO and geosynchronous Earth orbit (GEO) respectively. Typical launch vehicle concepts are illustrated in Figure 26. Mass properties, performance, and costs for these vehicles have been calculated in some detail. The results have consistently shown that transportation costs for these systems have been well within the range needed for SPS economic feasibility. (For example, \$20/kg to low Earth orbit versus an economic feasibility upper limit on the order of \$50/kg.) Low costs arise from (1) complete reusability; (2) high total traffic volume; (3) relatively rapid ground turnaround for relaunch; and (4) large payload capacity per flight —these factors are in order of importance to low recurring cost.

The identified advantages of each of the launch vehicle options are indicated in Figure 26. The principal issue between the two systems is sea landing versus land landing. The sea landing mode requires restart of some of the rocket engines (or start of special landing engines) for the powered letdown into the water. The vehicle is exposed to the sea saltwater environment. There is also some uncertainty associated with landing loads to be experienced upon water contact. The winged land landing vehicle avoids these issues. Because of the sonic boom profiles for ascent and reentry of the vehicles, and because the booster requires down range land landing, the winged system introduces significant launch and recovery siting issues. No suitable down range land landing sites are available for KSC launch. Possibly usable sites, with regions

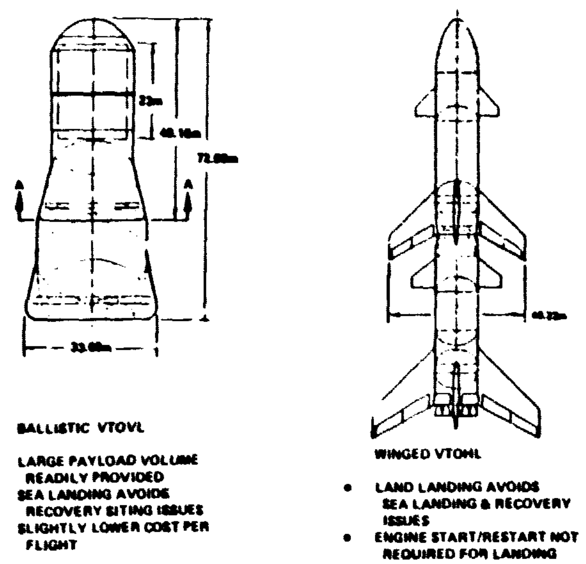

Figure 26. Launch System Options

of significant sonic boom overpressure being under government control, exist in the southwestern United States. These sites are further north than KSC and introduce additional performance penalties associated with the plane change required to achieve a zero-inclination geosynchronous orbit. Other alternative sites have not been identified.

The analyses of freight launch vehicles conducted during this study have indicated a low earth transportation cost on the order of \$20 per kilogram, including amortization of the vehicle fleet investment, total operations manpower, and propellant costs. The distribution of this cost over the assumed 14 year program is shown in Figure 27.

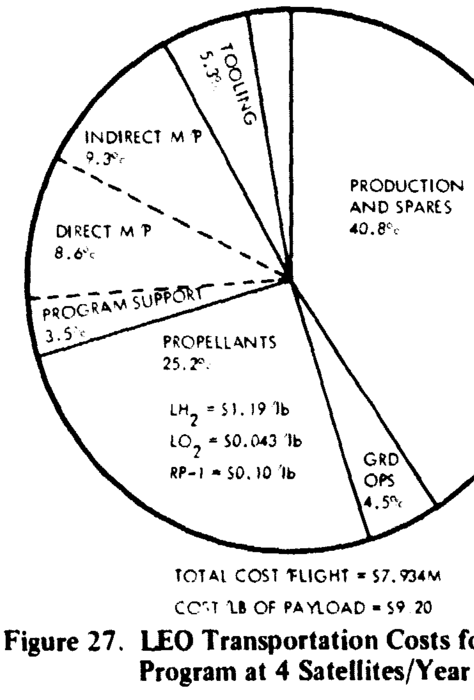

Figure 27. LEO Transportation Costs for 14 Year Program at 4 Satellites/Year

Vehicle production hardware is the greatest factor; manpower is second in importance, and propellants are third. The propellant cost is about 1/4 of the total, typical of a mature transportation system.

Since vehicle production is the most important component of space transportation costs, it is important to compare the estimates to other similar systems. Shown in Figure 28 are costs in terms of dollars per pound for several aerospace vehicles, including commercial aircraft and launch vehicles, as well as the calculated costs for the second stage and first stage of the winged launch vehicle systems. All costs here are expressed as the average costs over 300 units with appropriate learning curves applied. The commercial aircraft are similar in complexity to the launch vehicles, but involve a

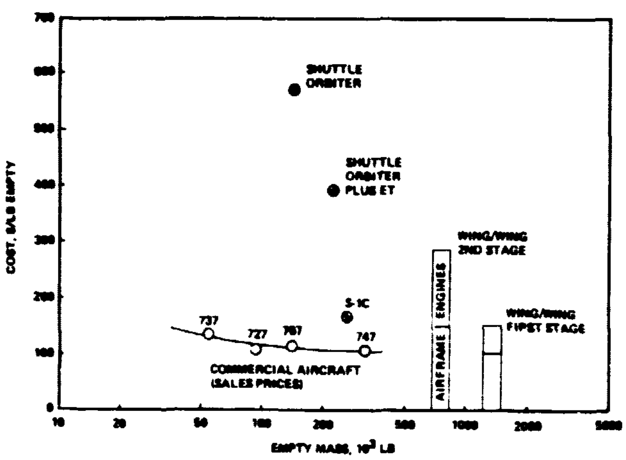

Figure 28. Flight Vehicle Production Hardware Costs

significantly smaller investment in propulsion. The S-1C Saturn booster stage is comparable in complexity to the first stage of the wing-wing vehicle. Shuttle costs are seen to be somewhat higher than would be expected from the cost estimates here. This differential arises primarily because Shuttle fabrication is being carried out with prototype rather than production tooling since only a few vehicles are to be built.

Transportation operations may be required to support construction operations either at low Earth orbit (LEO) or geosynchronous orbit (GEO), depending on which construction location is finally selected. In either case an orbit transfer vehicle system is needed to carry crews, crew resupply logistics, and priority cargo to geosynchronous orbit. Earlier studies had investigated a variety of orbit transfer vehicle options and selected the configuration illustrated in Figure 29 as representative of a cost-optimal system. It is a space-based oxygen-hydrogen reusable 2-stage rocket system refueled by tankers brought to LEO by the heavy lift launch system. During Part I of this study, the natural question arose, "why not make the tanker into an orbit transfer vehicle and operate Earth-based?". This was investigated, and it was found that the space-based vehicle had about 15% better performance, yielding lower costs. There are two primary reasons: (1) the space-based vehicle need not be structurally designed to withstand launch loads with full propellant tanks; (2) the inert mass of engines and other subsystems needed to make the tanker into a vehicle need not be hauled back and forth from Earth to LEO. Concurrent with this

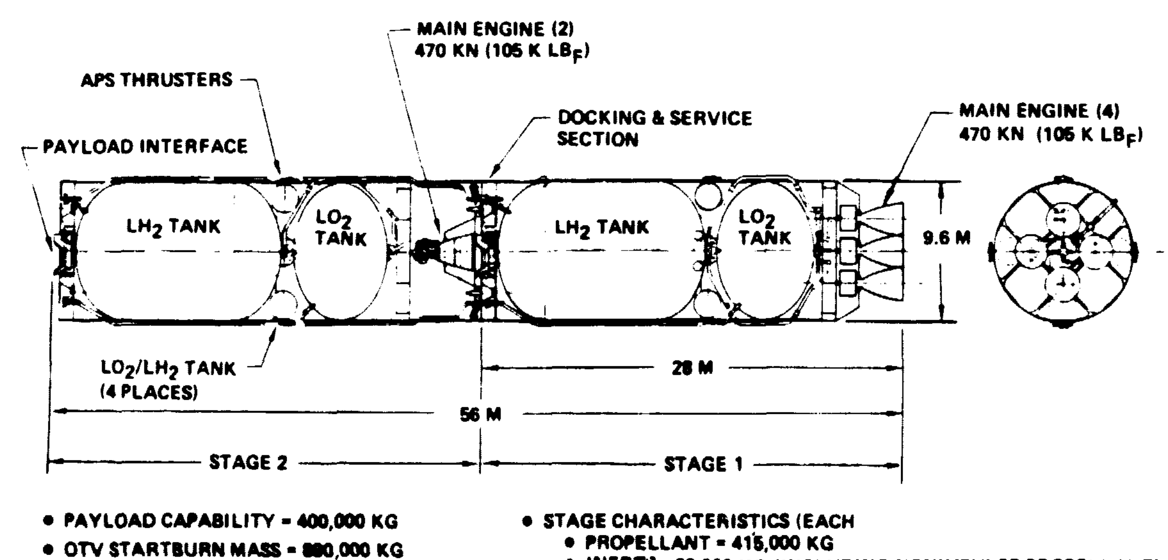

Figure 29. Space Based Common Stage OTV

SPS study, an orbital propellant depot study by General Dynamics has identified practical means of propellant transfer with minimal losses. The space-based system was selected as the preferred option.

If the SPS is constructed in low Earth orbit in a modular fashion, the electric generating capability of the modules may be used to drive electric propulsion systems to effect the orbit transfer. Each module is equipped with electric propulsion installations, propellant tanks, and the other subsystems necessary to convert it into a powered spacecraft. A joint cost optimization of Isp and trip time resulted in selection of a 180-day transfer at 7500 seconds electrical Isp. The effective Isp, after accounting for losses for attitude control thrusting and the use of chemical propulsion during transits of the Earth's shadow, is about 3000 seconds. This high effective specific impulse provides a major reduction in total freight delivery to low Earth orbit. The LO_2/LH_2 orbit transfer vehicle requires about 2.1 kg of propellant per kg of payload delivered to GEO. The high-specific-impulse option requires about 0.25 kg of propellant per kg of payload delivered. The net effect is a 50% reduction in the required number of heavy lift launches from Earth. There are a number of negative factors associated with the high specific impulse "self-powered" mode, but taken in the aggregate they exhibit considerably less cost than the savings in Earth launches.

The arrangment of a photovoltaic SPS module as a powered spacecraft is shown in Figure 30. One-quarter of the solar blankets are used for the transfer; the remainder are deployed from their shipping boxes after the module reaches geosynchronous orbit. The blankets used for propulsion power will be degraded by van Allen belt radiation absorbed during the transfer. They will be annealed

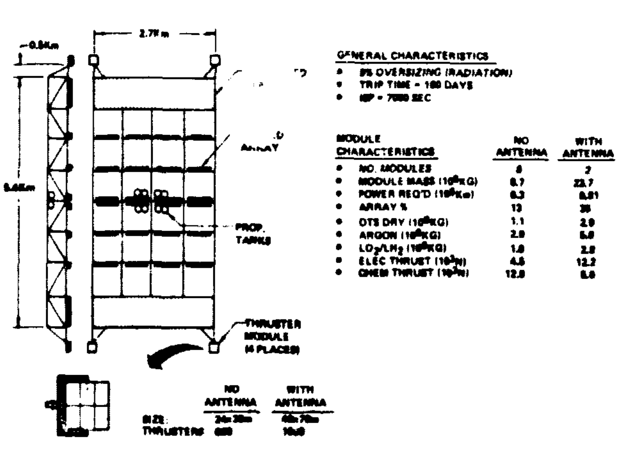

Figure 30. Self Power Configuration–Photovoltaic Satellite

during the final checkout and preparation process. Other tasks to be conducted at GEO include joining the modules together to form a complete SPS, and installing the antennas. The latter are also built at LEO, and are transported by two of the eight modules. Figure 31 shows a summary construction and transportation timeline.

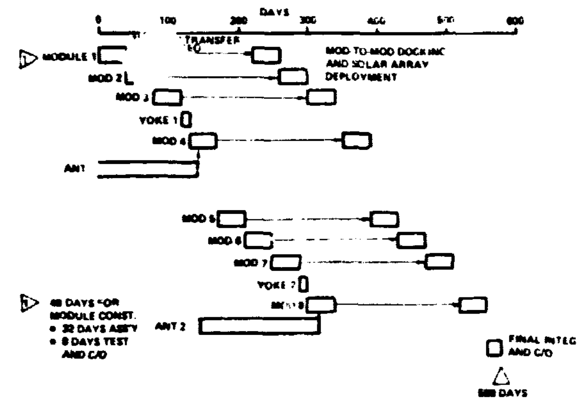

Figure 31. Photovoltaic Satellite–LEO Construction Timeline

Cost Analyses

One of the significant areas of emphasis of current SPS studies has been system costs, especially recurring (production) costs of SPS units to utilities. The present estimates of capital cost range from \$1700 to \$2700 per installed kilowatt (of useful ground output) for a modest-technology SPS system using silicon solar cells or potassium vapor Rankine heat engines (the latter, of course, employing solar concentrators). Since the installed kilowatts are baseload power rather than peaking or intermediate, the comparison with ground solar costs is potentially quite favorable.

These cost estimates may seem surprising. Since it is hardly obvious that putting a power plant in space will do anything to reduce cost, some explanations are in order.

Cost ultimately derives from the cost of materials, of energy and of value added during production and installation. The SPS scores well on the first and the last of these, and on energy investment, scores a little better than typical nuclear systems.

Materials

Constructed and operated in space where design loads are nearly absent, a typical 10,000 megawatt SPS will have a total mass of 100,000 metric tons, about that of the structure of a supertanker ship. Over 60% of the mass, be it a thermal engine or solar cell SPS, will energy collection

ORIGINAL PAGE IS OF POOR QUALITY

and conversion equipment with the balance being supporting structure, power transmitters, flight controls, and so forth. The energy conversion equipment provides several times as much output per unit area as a ground solar unit due to the continuous availability in space of sunlight of higher intensity.

Our SPS designs have employed very little in the way of exotic materials and are, except for their large size, relatively simple. The receiving antennas are also simple designs using ordinary materials (mostly concrete). With the receiving antennas included, the total materials required per kilowatt for an SPS are very similar to those for a conventional Earth-based plant: much less than for an Earth-based solar plant.

Energy

Lifetime energy investment to produce, install and operate an SPS is less than for most energy alternatives even if the latent energy in fuel for the alternatives is not counted. The energy cost of rocket propellant for space transportation has been calculated to be from 2000 to 4000 kw_{th} per kw_e installed: therefore, the payback time for rocket propellant is less than six months; less than two months if energy grade is included in the calculation.

Value Added

SPS systems and their receiving antennas are primarily made of simple, highly repetitive elements: billions of solar cells (or hundreds of thermal engine turbomachines): hundreds of thousands of standardized structural parts: tens of thousands of RF power tubes and associated circuitry: hundreds of standardized electrical switchgear units and power processors: billions of receiver dipole elements on the ground receiving antenna. All of these repetitive elements are well suited to highly automated mass production. This mass producibility is one of the keys to making SPS's at acceptable cost. Further, assembly of the SPS structure in space provides the unique opportunity to perform the assembly, even of this very large-area structure, in a semi-automated production line manner. This is true because the lack of gravity and wind loads allows moving the SPS with respect to the assembly facility with relative ease.

Cost Analysis Approach

In view of the mass production potentials, we have adopted a dual costing approach: For those items needed at production rates typical of aerospace products, we have used aerospace cost estimating practices. Fo: those items needed at mass production rates, we have used mass production cost estimating. The relationships are illustrated in Figures 32 and 33. Aerospace cost experience follows a "learning" or improvement curve. (Most of the improvement comes from learning how to make the production plan work. Mechanics learn quickly.) Typical experience is an 85% curve: unit #2N will cost 85% of unit #N. 727 jetliner production experience shows that this type of projection is good well beyond the 1000th unit. Aerospace estimates, built up from the subsystem level, are based on historical correlations of manhours, element physical characteristics, and complexity.

A mass production process is facility and equipment intensive rather than labor intensive. It does not follow an aerospace-type improvement curve. Historical correlations indicate a labor intensiveness relationship as shown in Figure 33. A mass productic . process reaches its labor cost plateau during the process shakedown period and then improves no further unless the process is changed.

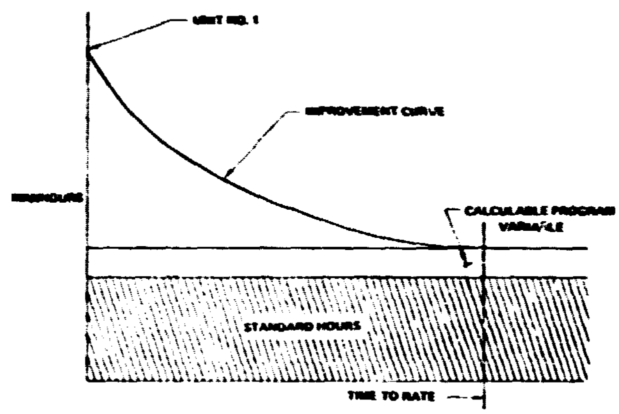

Figure 32. Cost Improvement Curve

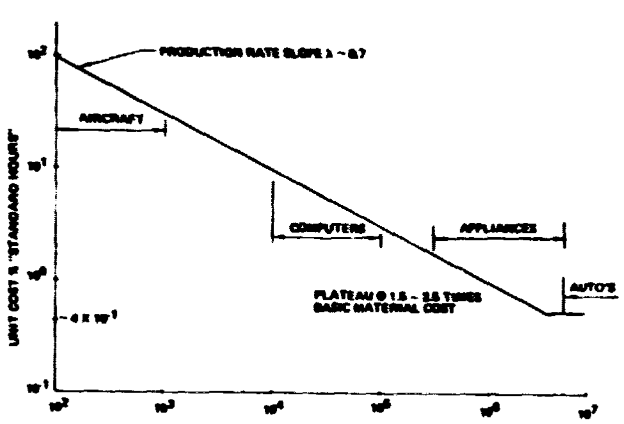

Figure 33. Mature Industry: Production Rate Curve

This mature industry costing approach was developed by Dr. Joe Gauger based on information developed during IR&D analyses of design-to-cost, experienced costs for commercial aircraft and other systems, and statistical correlations for financial and production factors for a wide variety of commercial industries.

It was judged to be desirable to spot-check the mature industry predictions. A total of five spot checks were made as indicated in Table 10. These included solar blankets, graphite structures, klystrons, potassium vapor turbines, and electromagnetic liquid potassium feed pumps. In all cases, the mature industry projection was well within the uncertainties that would be expected for the kind of cost estimates being made. Based on these examples, we believe the mature industry methodology to be an appropriate cost estimating procedure for SPS systems.

Primary emphasis in the current study effort has been directed to production and installation costs. Further efforts will investigate maintenance costs; the very preliminary estimates that have been made indicate that maintenance cost contribution to electric power cost will be comparable to that for conventional ground powerplants.

Table 10. Mature Industry Cost Confirmation

	MATURE INDUSTRY PROJECTION	INDUSTRY ESTIMATES
SOLAR BLANKETS	\$22 to \$37/m²	\$25 to [illegible]/m² (RCA, TI, GE, MOTOROLA)
GRAPHITE EPOXY STRUCTURE	[illegible]/kg	[illegible]/kg (BOEING)
KLYSTRONS	[illegible]/TUBE	\$1750 to [illegible]/TUBE (VARIAN)
TURBINES	[illegible] to [illegible]/kg	[illegible]/kg (GE)
PUMPS	\$75 to \$100/kg	[illegible]/kg (GE)

Results

Total production costs are summarized in Figure 34 for eight combinations of energy conversion system, production rate, and construction location. The silicon photovoltaic system has a modest cost advantage over the thermal engine and low Earth orbit construction has a significant cost advantage over geosynchronous construction. The most important cost change occurs with the production rate increase from 1 SPS per year early in the program, to 4 SPS's per year in a more mature operation. Principal cost reductions with system maturity occur in SPS hardware production, space transportation, and projected product improvement. The lower capital cost is achieved with the silicon photovoltaic system at 4 SPS's per year with LEO construction. The figure is approximately \$1,700 per kilowatt electric including interest during construction and projected growth. Still lower figures might be projected for advanced systems, such as thin film gallium arsenide.

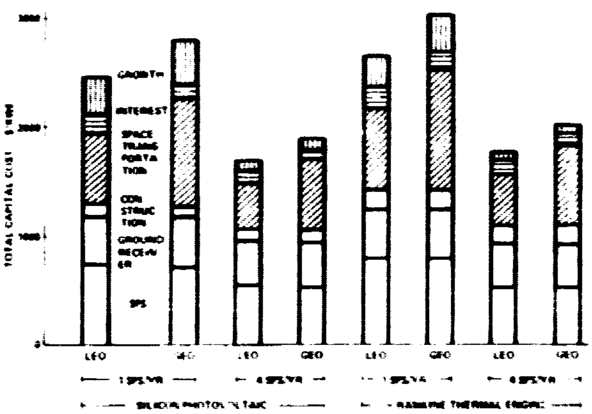

Figure 34. Production Cost Results Summary

Achievement of the projected silicon photovoltaic costs is critically dependent on the development of a satisfactory mass production technology for single crystal silicon solar cells and blankets. This mass production technology may require continuous growth processes but recent indications of improvements in the technology presently used for solar cell manufacture, indicate that automation of this technology may provide greater cost reduction than commonly supposed.

Uncertainty Analyses

An important objective of the SPS systems study was to make the best possible estimates of uncertainty in size, mass and costs, for the SPS systems characterized. The methodology employed was newly developed for the study. The basis for the uncertainty analyses was itemized estimates in the uncertainties of component performance, masses, and cost; a typical example is the uncertainty in solar cell efficiency and degradation. In developing the statistics in size, mass and cost, correlations were taken into account through the use of a bivariate normal distribution probability model.

The uncertainty analysis, in addition to estimating uncertainties, produced the unexpected result of predicting mass growth similar to that predicted by historical correlations. It had been believed that mass growth was the result of unpre-

dictable variables, e.g., changes in program requirements. The outcome of this uncertainty analysis suggests that growth is more predictable than formerly believed and in fact results largely from the natural tendency to set point design parameters on the optimistic side of the actual uncertainty range.

Figure 35 compares the statistically-derived result for the photovoltaic SPS with the worst-on-worst and best-on-best results defined by combining all the most optimistic component uncertainties and all the most pessimistic component performances. As increased detail is developed in this kind of analysis, the worst-on-worst and best-on-best extremes will continue to become further apart, while the statistical uncertainties will tend to change little and will approach a representation of true uncertainties. Significantly, the reference point design was outside the projected 3 sigma range for mass and size. This resulted primarily because the efficiency chain assigned to the reference design was more optimistic than the most probable efficiency chain defined by the statistical analyses.

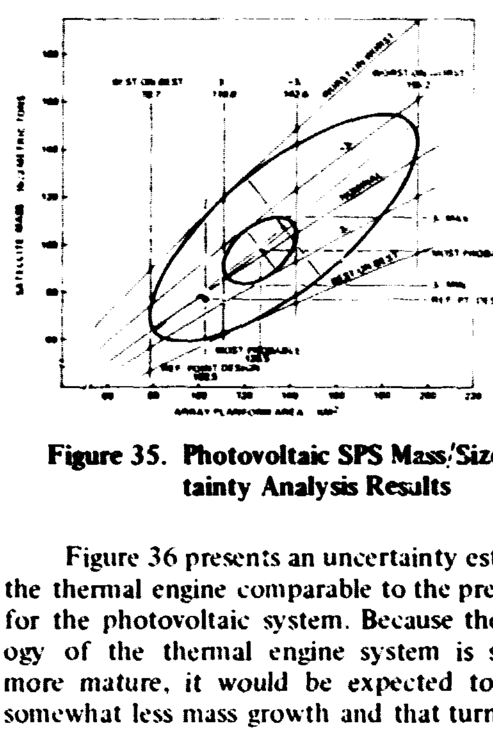

Figure 35. Photovoltaic SPS Mass/Size Uncertainty Analysis Results

Figure 36 presents an uncertainty estimate for the thermal engine comparable to the previous one for the photovoltaic system. Because the technology of the thermal engine system is somewhat more mature, it would be expected to estimate somewhat less mass growth and that turned out to be the case. An additional factor in the reduced mass growth projection is that a significant part of the size escalation is associated with the size of the concentrator which is a low-mass component of the thermal engine system.

With costs included in the uncertainty analyses, it is necessary to discriminate between the 1 SPS per year case and the 4 SPS per year case. For the 4 SPS per year case, an estimate was made that

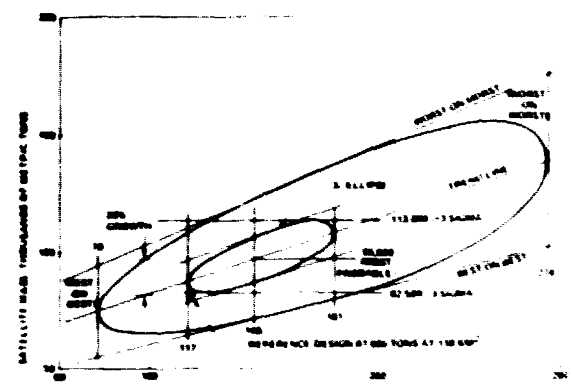

Figure 36. Thermal Engine Uncertainty Results

about 60% of the predicted mass growth could be removed by product improvement. As for the size and mass estimates, the reference design trended toward the optimistic side of the median of the cost uncertainties as shown in Figure 37. Consequently, one sees first a cost escalation at the reference design point and then a further cost growth associated with the mass growth projection. Note the very high correlation between cost and mass uncertainties. This corresponds to the historical indications that cost growth is frequently associated with mass growth, and especially with the compensation for (or removal of) mass growth in a system when performance requirements dictate that mass growth be limited to predetermined values.

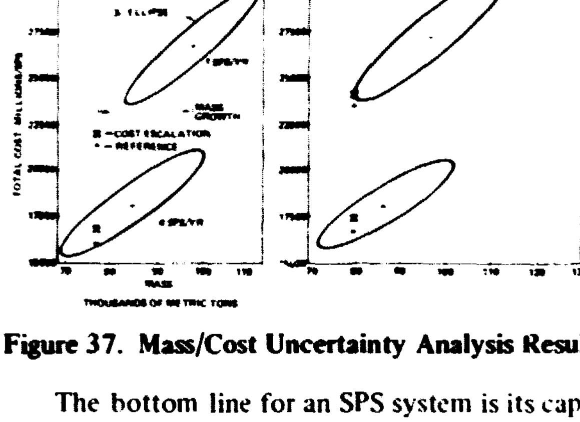

Figure 37. Mass/Cost Uncertainty Analysis Results

The bottom line for an SPS system is its capability to produce power at an acceptable cost. The result shown in Figure 38 represents the final result of the costing and uncertainty analyses. Uncertainties for busbar power costs include the uncertainties in unit costs as well as uncertainties in the appropriate capital charge factor to be applied and the plant factor at which the SPS can operate. Capital charge factors from 12-18 percent were considered and the plant factor uncertainty was taken as

70%-90% at one SPS per year and 85%-95% for four SPS's per year. These uncertainties were statistically combined with the cost uncertainties derived by the cost uncertainty analyses.

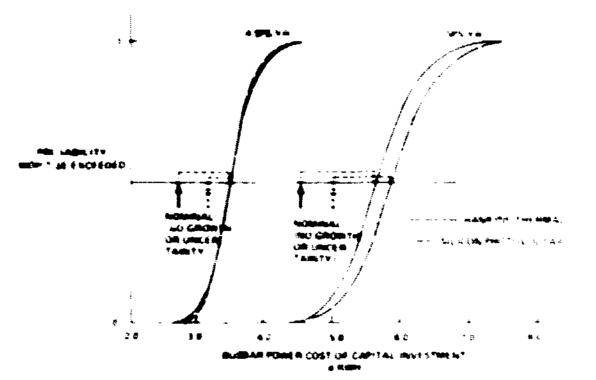

Figure 38. Predicted Busbar Power Cost and Uncertainties

Technology Verification Needs

Establishment of firm designs, performance levels, development requirements, cost estimates, and environmental acceptability, depends on the achievable characteristics of several critical technologies. Although overall success of SPS development is possible over a range of performance of these technologies, establishment of specific attainable performance levels is important to establishment of designs and system specifications. Accordingly, technology verification can presently be regarded as a schedule constraint for potential availability of SPS-derived energy. Initiation of a technology verification program is recommended as a logical addition to current SPS efforts. The ground-based program should lead the flight program by one to two years.

Ground-Based Technology Verification:

The recommended program includes energy conversion, materials, structures, electrical systems, RF systems, flight control, space transportation, space construction operations, and space environment effects, as summarized in Table 11.

Table 11. What Is Involved In Each Segment of the Verification Phase?

SPS FIVE YEAR GROUND BASED TECHNOLOGY VERIFICATION PROGRAM

- SOLAR BLANKETS (1ST YEAR FUNDING $2 5M 5 YEAR AGGREGATE $16M)
  - AUTOMATED SOLAR CELL BLANKET PRODUCTION
  - RADIATION EFFECTS INVESTIGATIONS
  - HIGH VOLTAGE ARRAY OPERATION
  - ADVANCED C L DEVELOPMENT
- THERMAL ENGINE DEVELOPMENT (1ST YEAR $2 5M, 5 YEAR AGGREGATE $16M)
- MATERIALS (1ST YEAR $1 5M, 5 YEAR AGGREGATE $10M)
  - PLASTICS AND COMPOSITES DEVELOPMENT FOR SPACE
  - LIFE AND PROPERTIES IN SPACE ENVIRONMENT
  - BONDING AND FASTENING TECHNIQUES FOR SPACE CONSTRUCTION
  - THERMAL CONTROL OF LARGE STRUCTURES
  - SPECIAL COATINGS AND ALLOYS DEVELOPMENT
- STRUCTURES (1ST YEAR $.75M, 5 YEAR AGGREGATE $8 75M)
  - FABRICATION AND TESTS OF STRUCTURAL AND JOINING ELEMENTS
  - ESTABLISHMENT OF METHODS FOR PREDICTING STRUCTURAL STRENGTH
  - STRUCTURAL DYNAMICS AND THERMAL RESPONSE
- ELECTRICAL SYSTEMS (1ST YEAR $1 5M, 5 YEAR AGGREGATE $12M)
  - DEVELOPMENT OF FAST SWITCHGEAR AND COMPONENTS FOR RF AMPLIFIER ARC SUPPRESSION
  - LIGHTWEIGHT AND HIGH EFFICIENCY POWER PROCESSORS
  - HIGH POWER SLIP RINGS
  - HIGH TEMPERATURE SEMICONDUCTORS
  - LIGHTWEIGHT ELECTRIC POWER STORAGE
- RF SYSTEMS (1ST YEAR $6M, 5 YEAR AGGREGATE $37M)
  - PERFORMANCE AND OPERATING CHARACTERISTICS
  - OVERALL SYSTEM DESIGN PARAMETERS AND COST ESTIMATES
  - DESIGN OF POWER TRANSMITTER AND INTEGRATION WITH ENTIRE SYSTEM
  - TECHNOLOGY VERIFICATION OF COMPONENT/SUBSYSTEM PERFORMANCES
  - DEVELOPMENT OF LABORATORY PROTOTYPE RF AMPLIFIER TUBES
  - PHASE CONTROL CIRCUITRY DEVELOPMENT
  - ANTENNA SUBARRAY HARDWARE
  - IONOSPHERIC HEATING TESTS
  - RADIO FREQUENCY INTERFERENCE TESTING
  - HIGH TEMPERATURE SOLID STATE AMPLIFIERS
  - DEVELOPMENT OF RECEIVING ANTENNA ELEMENTS
- FLIGHT CONTROL SYSTEMS (1ST YEAR $.5M, 5 YEAR AGGREGATE $4M)
  - DEVELOPMENT OF THEORY AND SOFTWARE TO CONTROL LARGE SPACE STRUCTURES
  - SENSOR DEVELOPMENT
- SPACE TRANSPORTATION (1ST YEAR $4M, 5 YEAR AGGREGATE $36M)
  - TECHNOLOGY VERIFICATION OF ZERO G PROPELLANT TRANSFER
  - HIGH POWERED ELECTRIC PROPULSION
  - NEW BOOSTER ENGINE TECHNOLOGY VERIFICATION
  - FULLY REUSABLE, WATER COOLED LAUNCH VEHICLE HEAT SHIELD
  - ON ORBIT SERVICING OF VEHICLES
  - TECHNOLOGY EFFORT FOR INITIATION OF DEVELOPMENT OF LOW COST TRANSPORTATION SYSTEM
- SPACE CONSTRUCTION OPERATIONS (1ST YEAR $3M, 5 YEAR AGGREGATE $22 5M)
  - AUTOMATED FABRICATION OF SPACE STRUCTURES
  - CLOSED LIFE SUPPORT SYSTEMS
  - DOCKING AND BERTHING OF LARGE SPACE SYSTEMS
  - DEVELOPMENT OF CONSTRUCTION OPERATOR ACCOMMODATIONS
  - CONSTRUCTION BASE ON BOARD LOGISTICS SYSTEMS
  - TECHNOLOGY VERIFICATION TO SUPPORT DEVELOPMENT OF CONSTRUCTION BASES
- SPACE ENVIRONMENT EFFECTS (1ST YEAR $2M 5 YEAR AGGREGATE $11M)
  - STUDY AND ANALYSIS OF SPACE ENVIRONMENT EFFECTS (METEOROIDS PLASMA FIELDS AND ENERGETIC RADIATION)

TOTALS FOR GROUND BASED TECHNOLOGY VERIFICATION PROGRAM

FIRST YEAR	$ 24 25M
AGGREGATE	$173 25M

Flight Test Technology Verification:

The recommended flight program is divided into two parts. The first phase includes an interferometer spacecraft experiment and shuttle sortie flights. The second phase is a solar power technology demonstrator in the power range 250 kw to 1000 kw, constructed and tended in low Earth orbit by the space shuttle. Costs for this program are less well defined: estimated totals are $50 to $100 million for the interferometer spacecraft, 675 million for shuttle sorties, and 2.1 billion for the solar power demonstrator including design, development, launches, construction, and the complete experiment program.